JKU

JOHANNES KEPLER
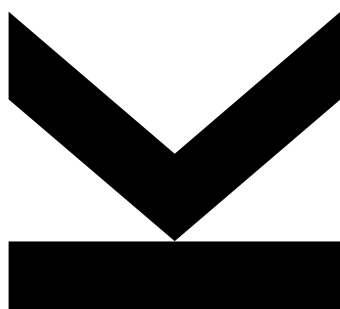**UNIVERSITY LINZ**

Submitted by
Kathrin Ebner

Submitted at
Linz Institute for Organic Solar Cells (LIOS) / Institute of Physical Chemistry

Supervisor
o.Univ. Prof. Mag. Dr. DDr. h.c. Niyazi Serdar Sariciftci

Co-Supervisor
Dogukan Hazar Apaydin MSc

October 2016

Silicon carbide electrodes for catalytic reduction of carbon dioxide

Master Thesis

to obtain the academic degree of

Diplom-Ingenieurin

in the Master's Program

Technical Chemistry

STATUTORY DECLARATION

I hereby declare that the thesis submitted is my own unaided work, that I have not used other than the sources indicated, and that all direct and indirect sources are acknowledged as references. This printed thesis is identical with the electronic version submitted.

……………………………….   ………………………………….

Place, Date   Signature

Abstract

In this thesis, the application of silicon carbide electrodes to address organometallic and biological catalysts for the electrochemical reduction of carbon dioxide to artificial fuels was investigated. Electrochemical conversion offers the possibility to avoid expensive co-factors or mediators that are often required as electron or proton donors in bio- or photocatalysis. Due to direct electron injection such co-factors become redundant. Additionally, electrochemistry opens the route towards renewable energy storage as solar or wind energy can be used as power sources. Moreover, the use of a semiconductor electrode offers the opportunity of prospective photoelectrochemical approaches.

As a biological catalyst, the enzyme formate dehydrogenase was tested in homogeneous as well as heterogeneous approaches. To immobilize the enzyme on the electrode, an alginate-silicate hybrid gel was employed as a matrix. The use of heterogeneous approaches by immobilizing the catalyst on the electrode presents the benefit of not needing any electron mediators due to enabled direct electron transfer. Moreover, catalyst reusability and separation from the product is facilitated.

CO_2 reduction with the organometallic benchmark catalyst Re(bipy)(CO)$_3$Cl at a silicon carbide electrode was studied as well. Said compound was not only employed as a homogeneous catalyst in organic solvents, but it was also shown that in a new approach the application of such can be realized in aqueous solution. This could be achieved by immobilizing the catalyst in the hybrid gel.

Kurzfassung

In vorliegender Arbeit wird die Anwendung von Siliziumkarbidelektroden zum Adressieren von biologischen und organometallischen Katalysatoren für die elektrochemische Reduktion von Kohlendioxid zu synthetischen Brennstoffen untersucht. Elektrochemische Umwandlung bietet die Möglichkeit teure Kofaktoren und Mediatoren zu vermeiden, welche bei bio- oder photokatalytischen Prozessen meist als Elektronen- oder Protonendonatoren erforderlich sind. Dank direktem Elektronentransfer sind diese Kofaktoren im elektrochemischen Prozess überflüssig. Darüber hinaus wird der Weg zur Speicherung erneuerbarer Energie eröffnet, da Solar- oder Windenergie als Stromquellen verwendet werden können. Die eingesetzten Halbleiterelektroden haben den zusätzlichen Vorteil, dass sie eventuell für zukünftige photoelektrochemischen Ansätze eingesetzt werden können.

Der erste Teil dieser Arbeit beschäftigt sich mit dem Einsatz von Formiatdehydrogenase als Katalysator sowohl in homogener als auch in heterogener Form. Um das Enzym auf der Elektrode zu immobilisieren wird es in ein Silikat-Alginat-Hybridgel eingebracht. Heterogene Katalyse bietet den Vorteil von direktem Elektronentransfer ohne Mediator als auch die leichte Abtrennung des Katalysators vom Produkt und daher die Möglichkeit der Wiederverwendung.

Im zweiten Teil wird der Fokus auf die Reduktion von CO_2 mit dem wohlbekannten organometallischen Katalysator Re(bipy)(CO)$_3$Cl gelegt. Gezeigt wird sowohl die homogene Anwendung der Verbindung in organischen Elektrolyten, als auch die heterogene Anwendung in wässrigem Elektrolyten in einem neuen Ansatz. Dafür wurde der Katalysator im Hybridgel an der Elektrode immobilisiert.

Table of Contents

1. Introduction

1.1. CO_2 reduction

In recent decades CO_2 levels have been constantly rising due to anthropogenic emissions. These excess amounts of the greenhouse gas CO_2 cannot be recycled in the natural carbon cycle.[1][2][3] Therefore it is necessary to find ways to address the problem by capturing and either storing and/or utilizing the greenhouse gas CO_2. However CO_2 is way more than a liability. It is crucial to change the general perception of carbon dioxide from an otiose contributor to climate change to a valuable widely available raw material and carbon source. Already at this point numerous options for CO_2 utilization exist. Examples are the use as an inert solvent, as a ligand in metalorganic complexes and as a reactant in chemical synthesis of base chemicals (see Figure 1) or polymers such as polycarbonates and polyurethanes just to name some.[1][2] Effort has to be made to implement these known processes in industrial applications to benefit of the possibility of simultaneously reducing the carbon footprint whilst making use of this important resource.[4]

However the utilization of CO_2 also presents some challenges: First of all CO_2 is a thermodynamically rather stable molecule with a ΔG_f^0 of -394.4 kJ mol^{-1}. Therefore converting CO_2 to high value C_1 or C_n products requires high energy input. Making these processes sustainable can only be achieved by using non carbon energy sources like wind or solar energy.[5][1] Secondly, also kinetics have to be considered. In reactions, where CO_2 is reduced (see Figure 1, C) and D)), the rate limiting step is believed to be the reduction of CO_2 to $CO_2^{\bullet -}$, where a change of hybridization of sp^2 to sp^3 and a bending of the former linear molecule occurs.[6] Also, when high energy is provided, side reactions become a significant problem.[5] To overcome these difficulties suitable catalysts are employed and a lot of work has been done in the field of catalyst research.[7][8][5][9][10][11][12]

In this work an electrochemical approach is used to yield CO_2 reduction products, mainly formate and CO. This presents the advantage of receiving high value chemicals while the requirement for generally expensive sacrificial electron donors vanishes. Additionally, processes can usually be carried out at room temperature and scaled up easily.[13] By providing the needed electricity from renewable energies, the process becomes sustainable. One, two, four, six and eight electron reduction processes can occur at an electrode to yield C_1 products. These processes as well as their corresponding formal potentials versus Normal Hydrogen Electrode (NHE) in aqueous media at a pH of 7 are given in Equation 1-7.[1][8]
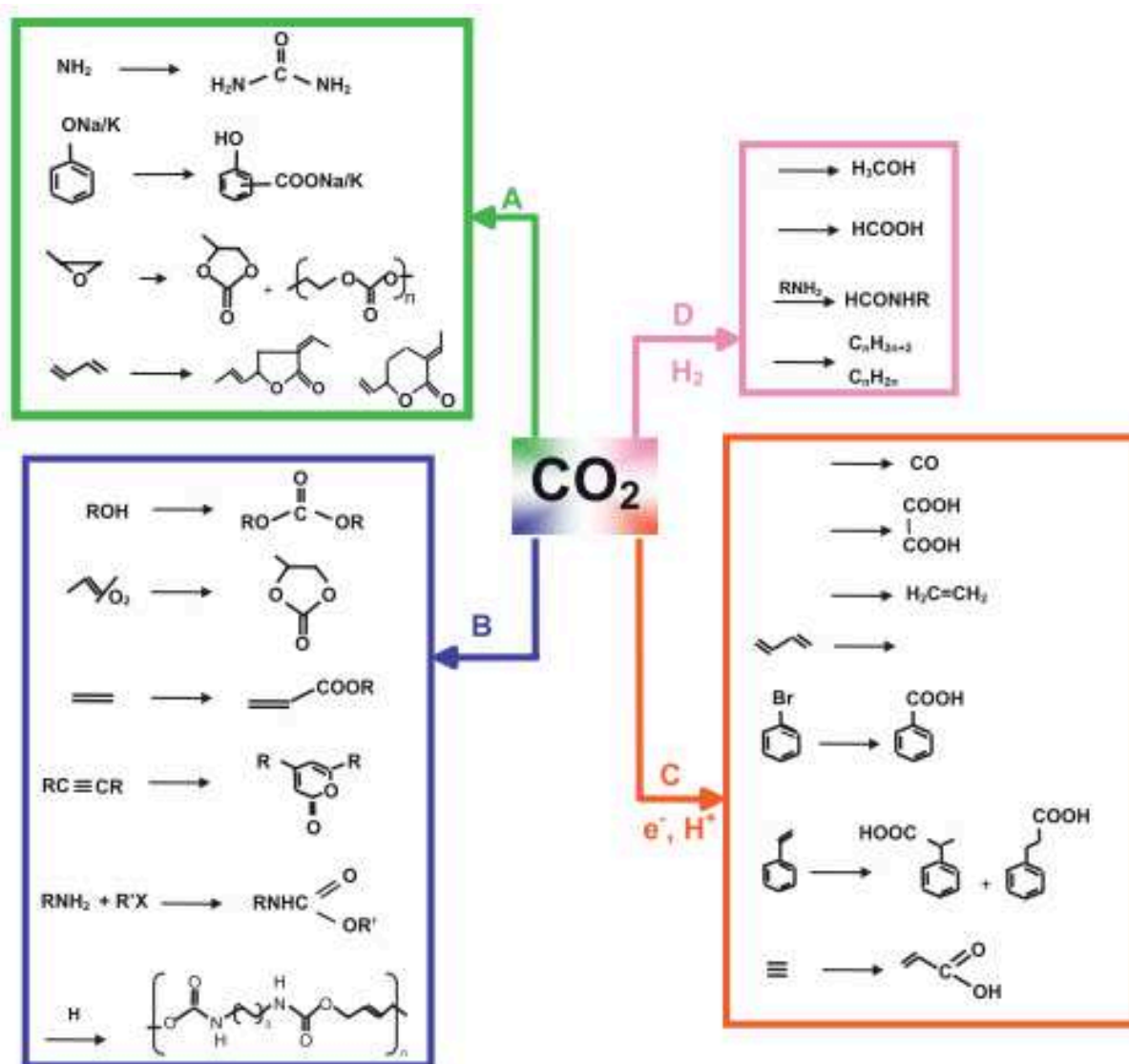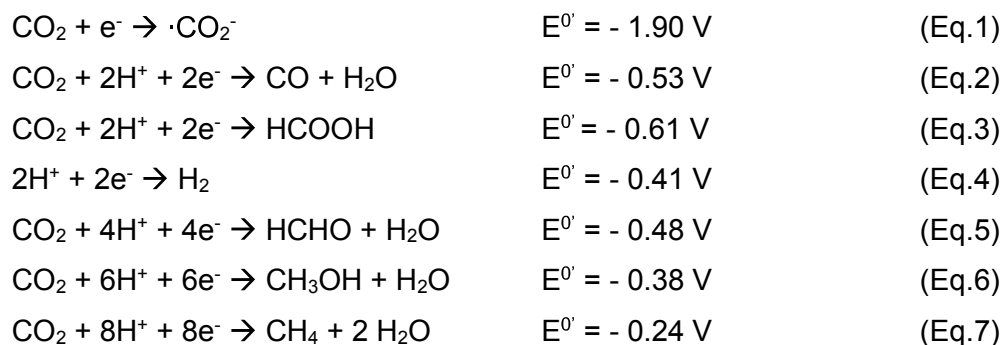
$$CO_2 + e^- \rightarrow \cdot CO_2^- \qquad E^{0'} = -1.90 \text{ V} \qquad (Eq.1)$$

$$CO_2 + 2H^+ + 2e^- \rightarrow CO + H_2O \qquad E^{0'} = -0.53 \text{ V} \qquad (Eq.2)$$

$$CO_2 + 2H^+ + 2e^- \rightarrow HCOOH \qquad E^{0'} = -0.61 \text{ V} \qquad (Eq.3)$$

$$2H^+ + 2e^- \rightarrow H_2 \qquad E^{0'} = -0.41 \text{ V} \qquad (Eq.4)$$

$$CO_2 + 4H^+ + 4e^- \rightarrow HCHO + H_2O \qquad E^{0'} = -0.48 \text{ V} \qquad (Eq.5)$$

$$CO_2 + 6H^+ + 6e^- \rightarrow CH_3OH + H_2O \qquad E^{0'} = -0.38 \text{ V} \qquad (Eq.6)$$

$$CO_2 + 8H^+ + 8e^- \rightarrow CH_4 + 2 H_2O \qquad E^{0'} = -0.24 \text{ V} \qquad (Eq.7)$$

Figure 1: Possible products from CO_2. A) and B) represent routes where the entire molecule is implemented. These reactions can occur at room temperature or lower. C) and D) represent routes where CO_2 is reduced to other products. Therefore additional energy is needed. Reproduced from [1].

As already mentioned the employment of catalysts is beneficial for higher selectivity and lowering

energy requirements. In the electrochemistry case this translates to lower overpotentials to the thermodynamic reduction potential. A general scheme for electrocatalysis is given in Figure 2. In this work, two catalysts have been investigated for the use with a silicon carbide electrode, namely the benchmark compound Re(bipy)(CO)$_3$Cl as first introduced by Hawecker, Lehn and Ziessel[12] and the enzyme formate dehydrogenase. A detailed introduction to those two catalyst systems is given in Section 1.2 and 1.3.
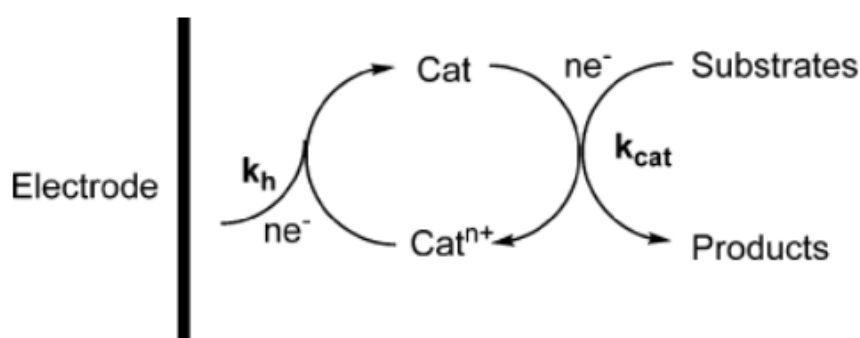

Figure 2: General scheme for electrocatalysis, where k$_h$ is the rate constant for the reduction of the catalyst at the electrode and k$_{cat}$ is the rate constant for the reduction of substrates to products. Reproduced from [8].

1.1.1. Formate/Formic Acid - a valuable product

In most experiments carried out in this work, formic acid (or formate depending on the pH of the electrolyte) is the main CO_2 reduction product. The reasons for targeting formic acid as a product are various: First of all, selling prizes are relatively high since production with industrial methods is costly.[13] Secondly, due to the two electron process for the reduction of formate, electricity consumption for the same product amount is lower than for e.g. formaldehyde, methanol or methane (assuming the same faradaic efficiency). Moreover the market for formic acid is expected to increase. In addition to the traditional applications for leather tanning, animal food or anti-icing agent several other technologies have been gaining importance in recent years:[13]

One of them is the use for hydrogen storage.[14][15][16] Formic acid can be decomposed to CO_2 and hydrogen releasing about 580 times more hydrogen than the same volume of pure hydrogen gas could deliver at standard conditions[13] - that equals to 4.4 w%.[16] Additionally, transporting and storing the liquid acid is way easier than the gaseous hydrogen. If the formic acid is produced by hydrogenation of CO_2, this technology is even sustainable.[14] Due to its efficiency, simplicity and sustainability this presents a viable route for energy storage.

Another application would be the direct use of formic acid in fuel cells. Formic acid was found to be a suitable fuel for powering fuel cells, which overcomes issues with the membrane known from methanol fuel cells as well as storage issues as one has to face working with hydrogen as a fuel. So called direct formic acid fuel cells (DFAFC) have shown excellent performance and are a promising candidate for a future power source.[17][18]

1.2. Enzymes as catalysts for CO_2-reduction

Enzymes offer several crucial advantages over other industrially applied catalysts:[19][20] First of all, reactions can usually be carried out in ambient conditions and the required energy is consequently low. Secondly, the solvent is mostly aqueous and therefore environmentally friendly. The enzyme itself is biodegradable and moreover it catalyzes the reaction very selectively towards one specific product and the need for cost- and labor-intensive product separation vanishes.

For the reduction of CO_2, depending on the targeted product many different enzymes can be employed. They all belong either to the class of oxidoreductases (e.g. formate dehydrogenase) or the class of lyases (e.g. carbonic anhydrase).[21]

Our group is focusing on a three step cascade employing dehydrogenases as catalysts (see Figure 3A) which has been proven to successfully produce methanol from CO_2.[22][23] In the first step, carbon dioxide is converted to formic acid catalyzed by formate dehydrogenase, subsequently formic acid gives formaldehyde catalyzed by formaldehyde dehydrogenase and lastly formaldehyde is converted to methanol with the help of alcohol dehydrogenase.[24] For all three steps, the sacrificial cofactor NADH is needed as an electron and proton donor. Unfortunately, NADH is a high price reactant and regeneration steps impair the overall efficiency.
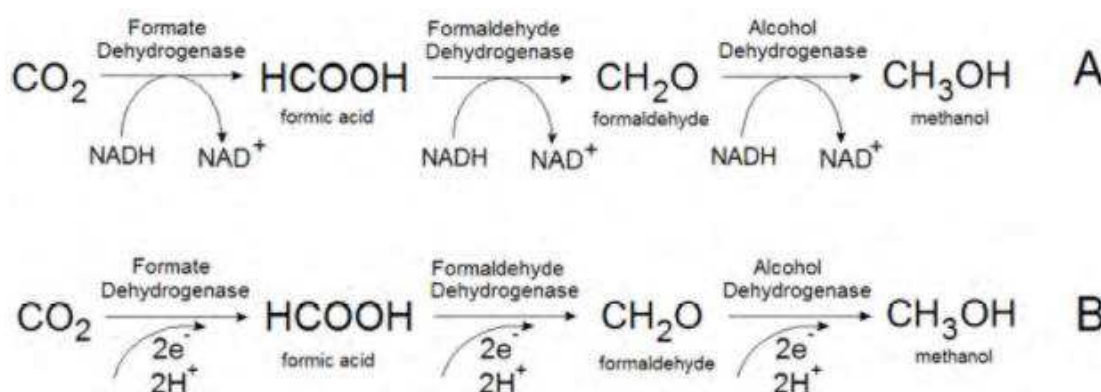

Figure 3: Mechanism for the reduction of CO_2 to Methanol in a three step cascade, A) with the sacrificial cofactor NADH, B) with direct electron injection. Reproduced from [24].

Therefore, efforts have been made to replace the cofactor by direct electron injection on an electrode.[25][24][26] To have the enzymes in close proximity to the electrode as well as to make use of the benefits heterogeneous catalysis has to offer, like reusability of the enzymes and facilitated product separation from the catalyst, Schlager et al immobilized the enzymes on the electrode in a alginate-silicate gel. [24][27] It has been known before that the gel works well for immobilizing enzymes as it has good diffusion characteristics for reactants and products while minimizing enzyme leakage. Also it has been proven that CO_2 can be reduced with the help of NADH in said matrix.[28] [23] However, in the new approach of Schlager et al, it could be shown that the cofactor could be completely replaced by direct electron injection (Figure 3B) through electrochemical processes when the enzyme was immobilized in the alginate-silicate hybrid gel. As a follow-up work, same was done on a silicon carbide electrode in present thesis, however only focusing on the first reduction step to formate.

1.3. Re(bipy)(CO)$_3$Cl as an electrocatalyst for CO$_2$-reduction

Re(bipy)(CO)$_3$Cl was first introduced by Hawecker, Lehn and Ziessel in 1984 and represented a benchmark compound in organometallic catalysis for CO_2 reduction.[29] The compound showed catalytic activity in photochemical and electrochemical approaches with the main product being CO. It was also found that the addition of protic solvents increased the catalytic performance of the catalyst however the mechanism was left unclear. The year after, the group of Sullivan published their findings on the mechanism, proposing two possible, independent pathways for the reduction of CO_2 shown in Figure 4.

fac−Re(bpy)(CO)$_3$Cl
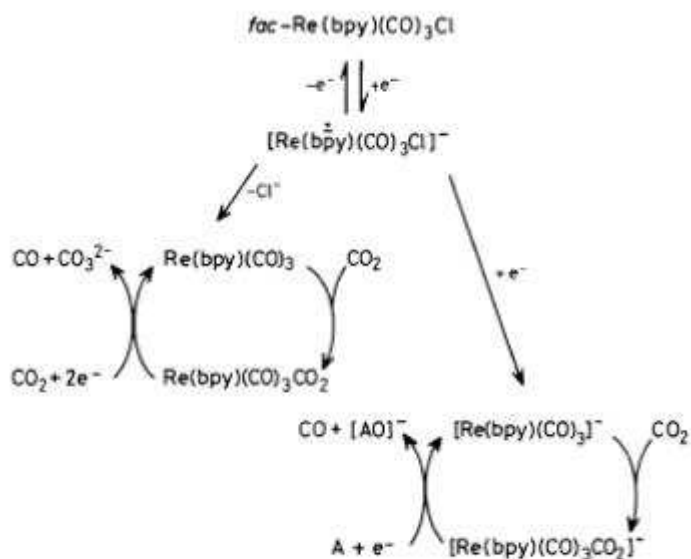
Scheme 1.
A = an oxide ion acceptor

Figure 4: Pathways for CO$_2$ reduction to CO published by Sullivan and coworkers. Reproduced from [30].

The characteristic features of the cyclic voltammogram of the compound are also shown by the authors (Figure 5).[30] Due to the fact that the potential of the first reduction wave is ligand-independent, authors concluded that this peak corresponds to a localized one-electron bipyridine reduction coupled to the formation of a dimer. Since there is no catalytic current at this potential in the presence of CO$_2$, one can assume that this reduction is not taking part in the CO$_2$ reduction mechanism as reflected in the two pathways in Figure 4.
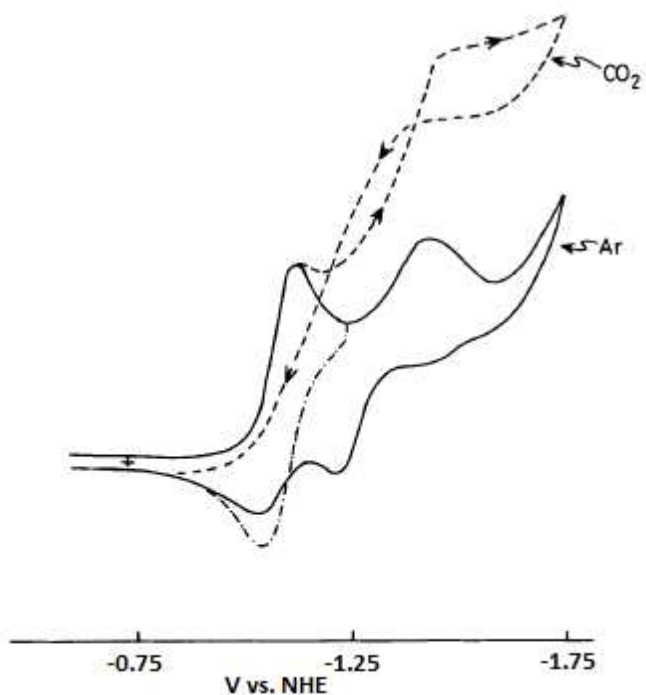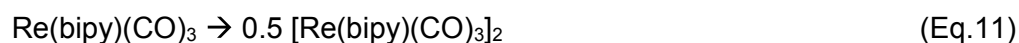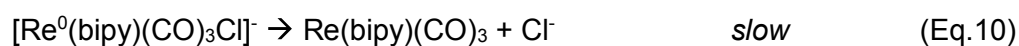
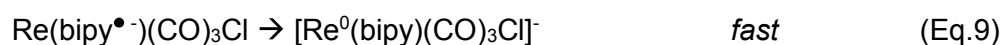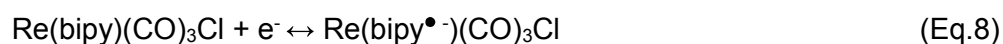Figure 5: Cyclic voltammogram of Re(bipy)(CO)$_3$Cl in an argon or CO$_2$ atmosphere. Reproduced from [30].

The mentioned dimer formation was further studied and the mechanism was proposed to be the following:[30]

$$Re(bipy)(CO)_3Cl + e^- \leftrightarrow Re(bipy^{\bullet -})(CO)_3Cl \qquad\qquad (Eq.8)$$

$$Re(bipy^{\bullet -})(CO)_3Cl \rightarrow [Re^0(bipy)(CO)_3Cl]^- \qquad\qquad fast \qquad (Eq.9)$$

$$[Re^0(bipy)(CO)_3Cl]^- \rightarrow Re(bipy)(CO)_3 + Cl^- \qquad\qquad slow \qquad (Eq.10)$$

$$Re(bipy)(CO)_3 \rightarrow 0.5\ [Re(bipy)(CO)_3]_2 \qquad\qquad (Eq.11)$$

Same was also found by Hawecker et al in 1986.[12] Moreover, the group investigated and published a possible mechanism for the formation of CO after addition of water to the organic solvent. It is shown in Figure 6.
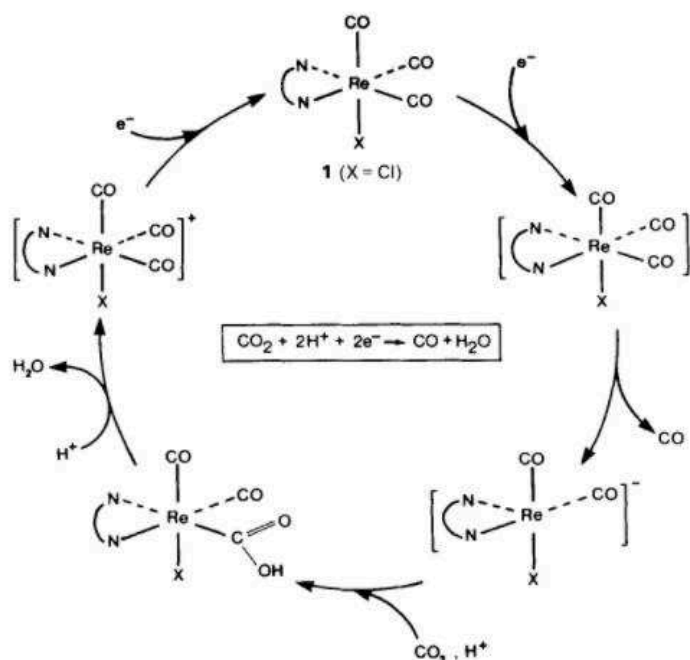
Figure 6: Catalytic cycle for the reduction of CO_2 to CO in the presence of water as suggested by Hawecker et al. X represents the coordinating anion, N-N the bipyridine ligand. Reproduced from [29].

In 1993, Yoshida et al succeeded in using the compound in pure aqueous solvent by immobilizing it in a Nafion membrane.[31] The formed products were CO and formic acid. The selectivity towards each product was influenced by the applied potential. As a side reaction, proton reduction occurred. Faradaic efficiencies were promising, however current densities were low due to low conductivity of the matrix.[32]

In present work, a new way of immobilizing the catalyst for application in aqueous solvents as well as homogeneous studies in acetonitrile with silicon carbide as an electrode material are shown.

1.4. Silicon Carbide

1.4.1. Physical properties of Silicon Carbide

A silicon carbide (SiC) crystal is formed by covalent bonds (sp^3-orbitals) between Si and C. In the crystal, each Si-atom is surrounded by four C-atoms and vice versa. Silicon Carbide exists in more than 200 different crystal structures (polytypes); the structure of the three most used ones is given in Figure 7. 3C-SiC is of the cubic primitive cell type, whereas all other forms are hexagonal.[33]
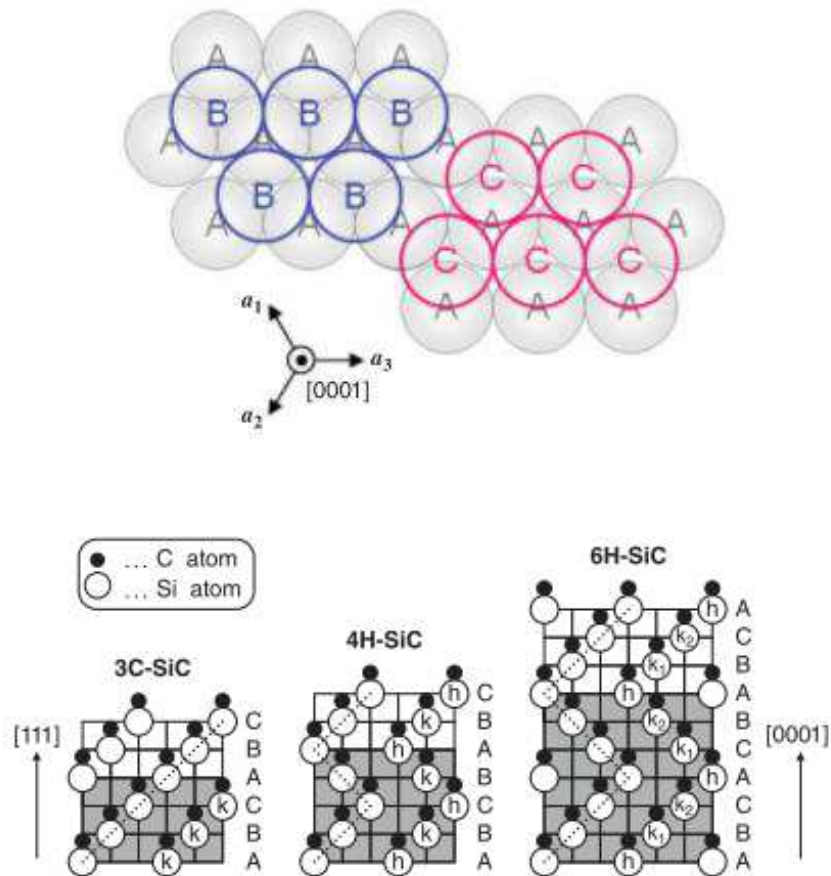
Figure 7: Different polytypes of SiC. Reproduced from [33].

Due to high bond energy (4.6 eV) SiC exhibits a variety of outstanding properties including high thermal, chemical and electrochemical stability. [33][34][35] Key data is given in Table 1.

	3C	4H	6H
Mohs hardness / -	9.2-9.3		
sublimation temperature / °C	>1800-2000		
specific heat capacity / J g^{-1} K^{-1}	0.69		
band gap / eV	2.36	3.23	3.02

Table 1: Most important properties of SiC.[34][33]

Silicon Carbide is a wide bandgap semiconductor, which can be easily doped. For n-doping nitrogen is usually employed while for p-doping mostly Al, sometimes also B is used.

1.4.2. Porous Silicon Carbide fabricated by a sol gel method

In 2007, Friedel et al introduced a new method for the fabrication of 3C Silicon Carbide: Conversion of graphite substrates by a sol-gel process. By that, the porosity of the product depends on the porosity of the substrate and can therefore be controlled rather easily. Doping is possible by introducing the dopants in the sol-gel via soluble precursors e.g. Nitrates (N) for n-doping or Borates (B) or Chlorides (Al) for p-doping respectively.[34][36][37][38]

The sol-gel itself is prepared by hydrolyzing and condensing TEOS in the presence of HCl and adding a certain amount of sucrose as carbon source. To receive the wanted granules, the sol is gelled and slowly dried under ambient conditions followed by annealing at 1000 °C under inert atmosphere.

For converting the substrates, the graphite as well as the granules are heated in a gradient furnace under argon to >1700 °C causing the granules to degrade. SiC vapor as well as gaseous CO and SiO forms, creating SiC seeds on which the crystals can then grow. The growth of the material continues until the precursor is fully consumed and can be repeated until the conversion is completed to the wanted extent. A more detailed description of the process can be found in literature. [34][36][37][38]

The obtained product is inexpensive, polycrystalline and already porous, without having to do cost-, material- and labor-intensive etching processes of wafers. It can be used for numerous applications[34] one of them being the application as an electrode as shown in this thesis.

1.4.3. Semiconductor electrodes

When a metal electrode is employed, electrons can easily move due to the available continuum of energy states and high electrical mobility. In semiconductors however, there is no such continuum. Band theory suggests that delocalized orbitals overlap resulting in a low- and a high-energy band, the valence band (VB) and the conduction band (CB). The energy zone between those bands (band gap (E_g)) is quantum mechanically forbidden. In intrinsic semiconductors, the VB is filled with electrons whereas the CB is empty due to the high energy needed to overcome the band gap.[39] Hole and electron density are equal in this case. To receive what is called a doped (extrinsic) semiconductor, impurities are introduced to the material causing excess electrons or holes respectively. The Fermi level (E_F), which is in the middle of the bandgap for the intrinsic case, will move towards the CB for n-type semiconductors and towards the VB for p-doped materials.[5]
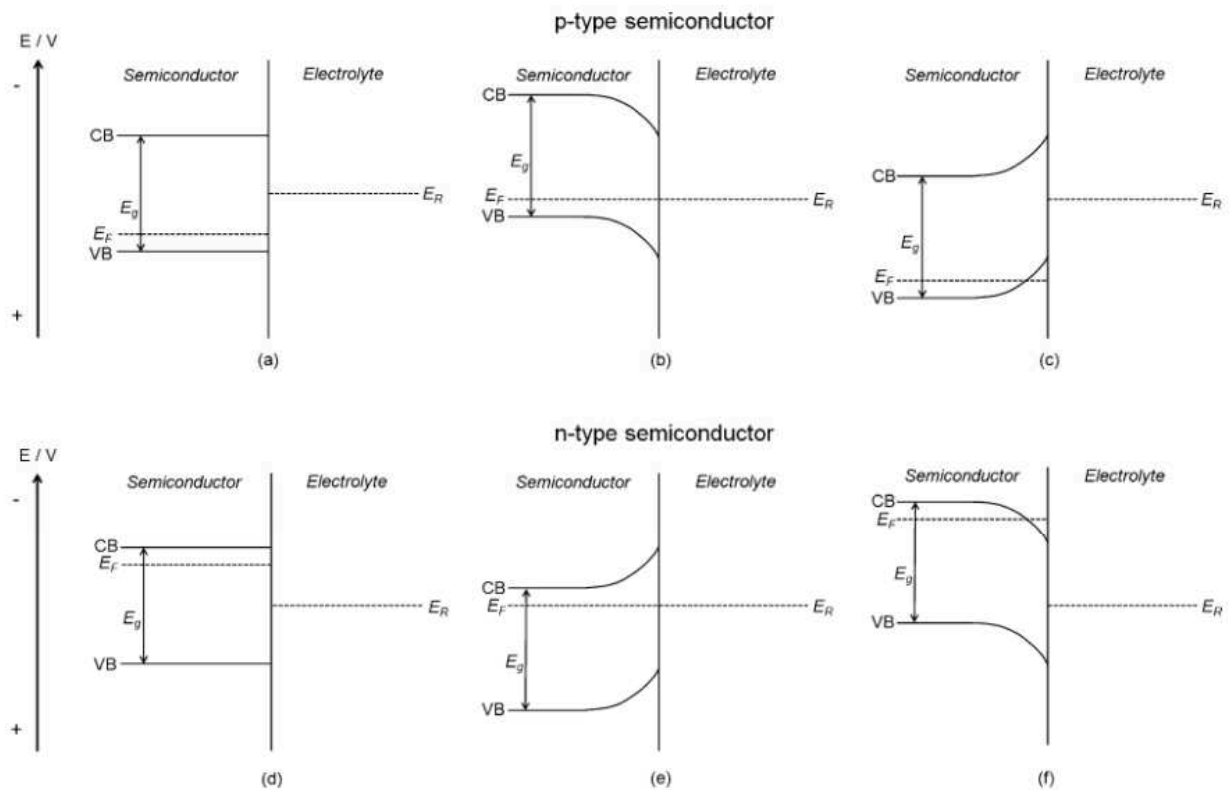
Figure 8: Band diagrams of semiconductors put in an electrolyte solution with the redox potential E_R. For the p-type case, see a-c; for n-type d-f. Diagrams before equilibrium are shown in a and d and after reaching equilibrium in b and e. Diagram c represents a p-type semiconductor with positive potential applied, while diagram f illustrates the n-type case with negative potential. Reproduced from [5].

When the semiconductor is now put in an electrolyte solution with the redox potential E_R, electrons will flow at the semiconductor-electrolyte interface to compensate for the difference in E_F and E_R. While E_R will stay about the same due to the amounts of electroactive species in the electrolyte, E_F will potentially move considerably causing also the CB and VB energies to shift with it in the proximity of the semiconductor-electrolyte interface (see Figure 8).[40] This process of depletion of the major carriers also creates the formation of a so called space-charge region in the semiconductor near the junction.[40][39] In Figure 8, it is also indicated that upon formation of the equilibrium band bending occurs in mentioned space-charge region resulting from a difference in occupied energy levels compared to the bulk material. Holes and electrons then move into different directions, one to the bulk and one towards the interface. Latter can be used to drive electrochemical processes on the semiconductor electrode.[5]

Upon application of an external potential, the shift of the Fermi level as well as the band bending will be reversed (Figure 8 c&f) due to the formation of an accumulation region. Therefore, the

charge carriers move in the exact opposite direction as described above for the equilibrium case (e.g. electrons towards surface for n-type semiconductor).[5,40][40]

The consequence is that n-doped semiconductors can be efficiently applied as either photoanodes or dark cathodes and p-doped materials as photocathodes and dark anodes respectively.[5][41][7][40] The application of the semiconductor SiC as a cathode is shown in this thesis.

2. Experimental

2.1. Materials

Chemicals and materials used for experiments are listed in Table 2.

Material/Compound	Supplier	Referred to as	Purity
Silicon carbide, polytype 6H	Xiamen Powerway Advanced Material Co.	6H-SiC	Research grade
Silicon carbide, polytype 4H	Xiamen Powerway Advanced Material Co.	4H-SiC	Research grade
Silicon carbide, polytype 3C	Bettina Friedel, TU Graz	porous SiC	-
Carbon felt	SGL Group	carbon felt	-
Acetonitrile	Roth	ACN	$\geq 99.9\ \%$
Formate dehydrogenase	Evocatal	$F_{ate}DH$	$\leq 0.4\ U\ /\ mg$
Alginic acid sodium salt	Sigma Aldrich	alginate	-
Tetraethylorthosilicate	Aldrich	TEOS	98 %
Tetrabutylammonium-hexaflurophoshate	Sigma Aldrich	$TBAPF_6$	$\geq 99.0\ \%$
Carbon dioxide	Linde	CO_2	99.995 %
Nitrogen	Linde	N_2	99.9990%
(2,2'-Bipyridine)-tricarbonylchlororhenium(I)	Gottfried Aufischer	$Re(bipy)(CO)_3Cl$	-
Trizma® base	Sigma Aldrich	TRIS	$\geq 99.9\ \%$
Hydrochloric acid	Merck	HCl	37%
Hydrofluoric acid	Sigma Aldrich	HF	$\geq 48\ \%$
Calcium chloride	Roth	$CaCl_2$	$\geq 98\ \%$
3-Amino-7-dimethylamino-2-methylphenazine hydrochloride	Sigma Aldrich	neutral red	$\geq 90\ \%$
Platinum wire and foil	Alfa Aesar	Pt	99.9%
Silver wire	Roth	Ag	$\geq 99.9\ \%$
Acetone	VWR Chemicals	acetone	100%

Chloroform	VWR Chemicals	$CHCl_3$	99.3&%
Ethanol	Merck	EtOH	absolute
Ammonia	Merck	NH_4OH	25 %
Hydrogen peroxide	Merck	H_2O_2	30 %
Sodium Sulfate	Sigma Aldrich	Na_2SO_4	≥ 99.0 %
Sodium hydroxide	Sigma Aldrich	NaOH	≥ 98 %
Hydrogen	Linde	H_2	99.9990%
Helium	Linde	He	99.9990%
synthetic air	Linde	-	99.9990%
β-Nicotinamide adenine dinucleotide hydrate	Sigma Aldrich	NAD^+	≥ 98 %
Sodium formate	Sigma Aldrich	-	≥ 99.0 %
Polymethylmethacrylate	Sigma Aldrich	PMMA	-
Nickel	Alfa Aesar	Ni	99.98%
Argon	Linde	Ar	99.9990%
Chlorobenzene	Acros	-	99%

Table 2: Materials used for experiments.

2.2. Apparatus

Electrochemical measurements were performed on a Jaissle 1030 PC.T potentiostat/galvanostat. Pure water with a resistance 18.2 MΩ cm ($\triangleq$ 0.055 µS cm^{-1}) was obtained from a TKA-Genpure water purifying station. Hall measurement was carried out on a Lake Shore Cryotronics 8400 Series system.

For the detection of formate a Dionex ICS-5000 ion chromatograph was used. The amounts of hydrogen, methane and carbon monoxide were determined with a Thermo Scientific Trace GC Ultra gas chromatograph and the amounts of methanol on a Thermo Scienftific Trace 1310 gas chromatography system respectively. For a more detailed description of the analytical equipment, see section 2.3.

UV-Vis absorption measurements were performed with a Perkin Elmer Lambda 1050 system.

Nickel was evaporated at a Univex 350 setup and annealed in a Stöhlein Instruments CTF 12/65 tube furnance.

For electrochemical experiments under illumination, a Philipps halogen lamp (50 W, 12V) was used with a Delta Electronica SM6020 Power Supply and light intensity was adjusted to 60 mW cm^{-2} with a calibrated Si diode.

2.3. Analytical Methods

2.3.1. Gas Chromatography

2.3.1.1. Gas Chromatography with injection of gaseous sample

For analysis of H_2, CO or CH_4, 2 mL samples were taken from the headspace with a gastight syringe and injected manually in a Thermo Scientific Trace GC Ultra gas chromatography system. The temperature program of the oven is given in Table 3. The carrier gas for the left channel (detection of CO) is N_2 and for the right channel (detection of H_2 and CH_4) He respectively. Carrier gas flow is constant at 20 mL min^{-1}. The detector is a thermal conductivity detector (TCD) which is kept at 200°C.

rate / °C min^{-1}	temperature / °C	hold / min
	30	2
10	130	8

Table 3: Temperature program of the GC oven for injection of a gaseous sample.

2.3.1.2. Gas Chromatography with injection of liquid sample

The samples were analyzed with a Thermo Scientific Trace 1310 gas chromatograph with splitless liquid injection and a TR-WAX column (length: 30 m, inner diameter: 0.32 mm, film thickness: 0.50 µm). As carrier gas helium was used, the flow rate is 1.5 mL min^{-1}. The injection volume is 1 µL and the injector temperature is 260 °C. The temperature program of the oven is given in Table 4. For detection a flame ionization detector (FID) is employed at a temperature of 260°C.

rate / °C min^{-1}	temperature / °C	hold / min
	50	1
20	250	10

Table 4: Temperature program of the GC oven for injection of a liquid sample.

2.3.2. Ion Chromatography

For the detection of formate a Dionex ICS-5000 ion chromatograph equipped with a Dionex Ionpac AS19 column was used. The column temperature is 30 °C. The eluent is KOH, its concentration is given in Table 5.

time / min	concentration of KOH / mM
0	10
7	60
12	10

Table 5: KOH concentration in the IC eluent.

2.4. Ohmic Contacts

2.4.1. Preparation of Ohmic Contacts to 6H- and 4H-SiC wafers

For preliminary cleaning the substrates were sonicated in chloroform at room temperature for 10 min and subsequently rinsed with purified water. This procedure was repeated in acetone and ethanol. For native oxide removal, samples were etched for 10 min in 5 % HF at ambient conditions. After rinsing with purified water, samples were put in $NH_4OH:H_2O_2:H_2O = 1:1:5$ for 10 min at 70 °C and subsequently in $HCl:H_2O_2:H_2O = 1:1:5$ applying the same conditions (10 min, 70 °C). After evaporating 200 nm of Ni and annealing at 1000 °C under Argon atmosphere for 5 min ohmic contacts were formed. [42][43] Contacted samples can be seen in Figure 9.

2.4.2. Ohmic Contacts to porous 3C-SiC substrates

Since only the outer layer of the graphite substrate which is used as a precursor material for the sol gel process is converted to 3C-SiC, the sample can be contacted by scratching off said layer. The consequently exposed graphite can be contacted with platinum wire. To avoid direct contact of the electrolyte, the area is sealed with PMMA ($M_w = 350\,000$) solution (50 mg mL^{-1} in chlorobenzene). A contacted sample is shown in Figure 9.

Figure 9: a) 6H-SiC (left) and 4H-SiC (right) with annealed Nickel contacts, b) contacted 3C-SiC sample.

2.5. Characterization of wafers

2.5.1. Spectroscopic Characterization

The absorption spectrum of 6H- and 4H-SiC was recorded between 350 nm and 800 nm with a Perkin Elmer Lambda 1050 spectrometer. In the double beam spectrometer, the samples as well as air as a blank were measured and the resulting sample spectrum was baseline corrected. As a light source a tungsten lamp for visible light was employed and a deuterium lamp for UV light respectively. Transmitted light was detected by a photomultiplier tube, an InGaAs detector and a PbS detector.

2.5.2. Electrical Characterization

To determine the doping concentration of the wafers and to prove the formed contact to the wafers to be ohmic, Hall measurement as well as an ohmic check were performed at a Lake Shore Cryotronics 8400 Series system. The sample preparation and contacting was carried out as described in 2.4.1. The arrangement of contacts is depicted in Figure 10.

0.50 cm
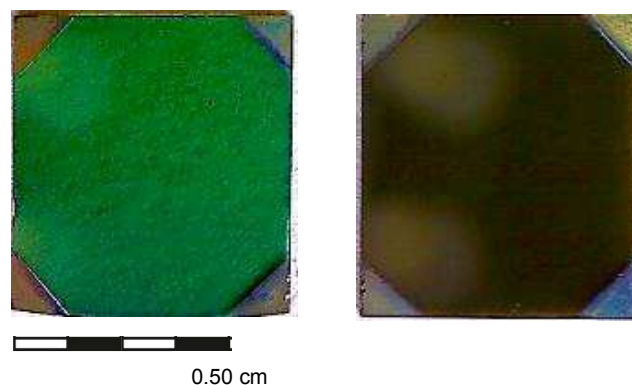
Figure 10: Samples for Hall measurement and ohmic check with four triangular Nickel contacts.

The thickness of the samples was determined to be 0.35 mm. The parameters for the AC Hall measurement were as follows: The excitation field frequency amounts to 50 mHz while the excitation current was 1 mA. The measurement was performed at ambient temperature at a field of 0.6370 T. For the ohmic check, ten points between a current of 10 μA to 100 μA were measured with linear spacing and from high to low current in positive and negative bias.

2.5.3. Electrochemical characterization

Experiments for electrode characterization were carried out in a one compartment cell as schematically depicted in Figure 11.[44] As working electrode SiC was employed while Platinum was used as the counter electrode. Depending on the electrolyte, the internal reference was either and Ag/AgCl in 3 M KCl or an Ag/AgCl - quasi-reference electrode (QRE) (for preparation and calibration see section 2.5.3.1.). Cyclic voltammetry was measured in the N_2 or CO_2 saturated system with applied potentials between 0 and -1400 mV vs. the reference electrode with a scan rate of 25 mV s^{-1}. The system was characterized in the dark and under illumination with a halogen lamp. As electrolytes 0.1 M Na_2SO_4 (pH = 7) was either employed as it is or titrated with HCl or NaOH to a pH of 4 or 10 respectively. For characterization at a very low pH, 0.1M HCl was used. To characterize the electrodes in organic medium as well, acetonitrile with 0.1M $TBAPF_6$ was utilized as an electrolyte solution.
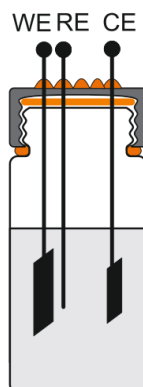
Figure 11: Schematic drawing of a one compartement cell (CE…Counter Electrode, RE…reference electrode, WE…working electrode). Reproduced from [44].

2.5.3.1. Preparation of the quasi reference electrode

As an internal reference in all experiments conducted in organic solvents an Ag/AgCl-quasi reference electrode was used. These electrodes were prepared by anodizing Ag. Therefore an Ag wire was polished and employed as the working electrode in a three electrode setup with a Pt counter electrode and an Ag/AgCl (3 M KCl) reference electrode. As an electrolyte 1M HCl was used. First, the potential was cycled ten times between 0 and 700 mV with a polarization rate of 10 mV s^{-1}. Next, the potential was held at 500 mV for 2 min and subsequently at 700 mV for 10 min. The wire was then rinsed with 18.2 MΩcm water and dried. Afterwards the QRE was calibrated against ferrocene/ferrocenium (Fe/Fe$^+$).

2.6. Homogeneous Enzyme Catalysis

Formate dehydrogenase, an enzyme catalyzing the two electron reduction of CO_2 to formate (see section 1.2.), was employed as a homogeneous catalyst in a two compartment electrochemical cell. As depicted in Figure 12, platinum was used as the counter electrode, Ag/AgCl (3 M KCl) as a reference and either 4H, 6H or porous 3C-SiC as the working electrode. 20 mg of enzyme (0.4 U mg^{-1}) were dissolved in 25mL TRIS-Buffer (0.05 M, pH=7.88 adjusted by titration with 3M HCl) under strict exclusion of oxygen. This solution was then used as electrolyte.

After the system was saturated with N_2 or CO_2 respectively, it was characterized by cyclic voltammetry. Potentials between 0 and -1400 mV and a scan rate of 5 mV s^{-1} were applied. Controlled potential electrolysis was performed for 3 h at a potential of -1200 mV and the production of formate was monitored with ion chromatography.
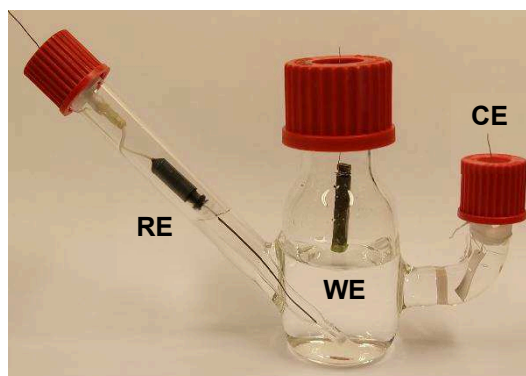
Figure 12: Photograph of a two compartment cell (WE: porous SiC, RE: Ag/AgCl (3 M KCl), CE: Pt).

2.6.1. Enzymatic Activity Test

Enzymatic activity testing was performed according to literature [45]. The procedure was however modified for the use of TRIS-buffer and ambient conditions, since the activity of the enzyme in the given environment in the electrochemical cell was of interest. Therefore the following solutions were prepared freshly: A) TRIS-buffer (0.05 M, pH=7.88 adjusted by titration with 3M HCl), B) 200 mM sodium formate in 18.2 MΩ cm water, C) 10.5 mM β-NAD in 18.2 MΩ cm water, D) 1.5 mM β-NAD in TRIS-buffer and E) 0.4 U / mL formate dehydrogenase in D). Then, the test and the blank sample were prepared by pipetting the given reagent volumes (Table 6) into quartz cuvettes. The UV-Vis absorption of both samples was measured after 0, 1, 2, 3, 4 and 5 minutes as described in 2.5.1. For baseline correction, the absorption spectrum of 18.2 MΩ cm water was used.

reagent	mL pipetted for test	mL pipetted for blank
18.2 MΩ cm water	1.10	1.10
A	0.75	0.75
B	0.75	0.75
C	0.30	0.30
D	-	0.10
E	0.10	-

Table 6: Volumes of reagent solutions needed for enzymatic activity testing.

2.7. Heterogeneous Enzyme Catalysis

An alginate-silicate hybrid gel, which is known from literature to be a good matrix for enzyme fixation[28][23][24], was used for immobilizing formate dehydrogenase on SiC-electrodes. All heterogeneous enzyme experiments were performed with porous 3C-SiC since the surface of the wafers is not an ideal substrate for the matrix, due to very low roughness. In preliminary experiments, the matrix delaminated from the wafers within seconds. To achieve optimal compatibility of the matrix with the underlying porous 3C-SiC substrate and prevent delamination, alginate concentrations between 2 and 4 w% were tested. It was found to be the optimum to dissolve 75 mg alginic acid sodium salt in 1 mL 18.2 MΩ cm water, add 0.5 mL TEOS and then stir vigorously. After 10 min stirring the upper phase of the arising two phase system, the surplus TEOS not incorporated in the alginate, was discarded. In the glove box 4 mg of formate dehydrogenase (0.4 U/mg) were dissolved in 0.5 mL TRIS-Buffer (0.05 M, pH=7.88 adjusted by titration with 3M HCl) and added to the matrix. After subsequent dipping of the electrode in said matrix and storage in 0.2 M $CaCl_2$ for 20 min to obtain sufficient crosslinking, the working electrode (Figure 13) could be employed in a three electrode setup in a two compartment cell as can be seen in Figure 12. As an electrolyte TRIS-Buffer was used, as counter electrode platinum and the internal reference was an Ag/AgCl (3 M KCl) electrode.

Cyclic voltammetry was performed after the system was saturated with N_2 or CO_2 respectively. Potentials between 0 and -1400 mV and scan rates of 5 or 25 mV s^{-1} were applied. For electrolysis, the potential was held at -1200mV for 3h and the production of formate was monitored by ion chromatography.

Figure 13: Enzymes immobilized on porous SiC electrode.

2.8. Homogeneous Catalysis with Re(bipy)(CO)$_3$Cl

All experiments in which Re(bipy)(CO)$_3$Cl was employed as a homogeneous catalyst were carried out in a one compartment cell as schematically depicted in Figure 11. As electrodes SiC (WE), Platinum (CE) and an Ag/AgCl - quasi-reference electrode (QRE) (for preparation and calibration see section 2.5.3.1.) were used. The supporting electrolyte was 0.1 M TBAPF$_6$ in acetonitrile, the catalyst concentration was $\cong$ 1mM. Cyclic voltammetry as well as electrolysis were performed after saturating the solution with N$_2$ or CO$_2$ respectively. CV was measured at a scan rate of 40 mV s^{-1}. Products formed during 3 h electrolysis at - 1600 mV were analyzed with GC and IC.

2.9. Heterogeneous Catalysis with Re(bipy)(CO)$_3$Cl

As a novel way of heterogeneous catalysis with Re(bipy)(CO)$_3$Cl in aqueous solution, the catalyst was immobilized in the alginate-silicate hybrid gel matrix known from immobilization of enzymes (see section 2.7.) [28][23][24]. Therefore 4 mg of Re(bipy)(CO)$_3$Cl was dispersed in 0.5 mL TEOS and in a separate vial 75 mg alginic acid sodium salt was fully dissolved in 1.5 mL 18.2 MΩ cm water. In the next step, both liquids were combined and upon vigorous stirring the catalyst got incorporated in the matrix. This process could be easily monitored by tracking the color change of the upper (TEOS) and lower (hybrid gel matrix) layer, since the catalyst itself is of bright yellow color. After mixing, the upper layer representing surplus TEOS was discarded. Subsequently the electrode was soaked in the matrix. After 20 min storage in 0.2 M CaCl$_2$ for crosslinking the electrode is ready for employment in an electrochemical cell. Again, only porous 3C-SiC could be used as a substrate, since the matrix is not compatible with the wafer surface and delaminates within seconds. The preparation process of the matrix can be seen in Figure 14.
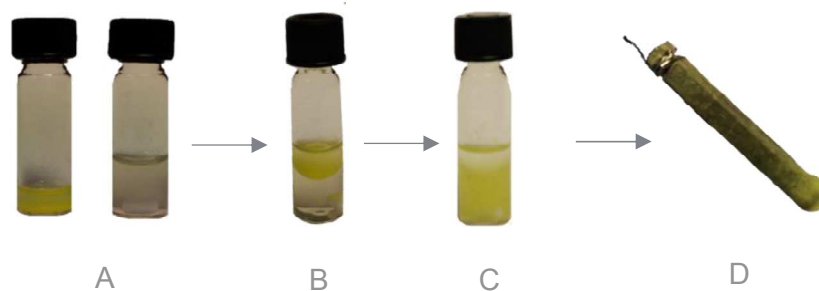
Figure 14: A) Re(bipy)(CO)₃Cl in TEOS and alginate matrix, B) both combined but not yet mixed, C) upon vigorous stirring the catalyst gets incorporated into the matrix, D) the electrode covered with immobilized catalyst.

Electrochemical characterization was done in a two compartment cell. The three electrode setup consisted of the $Re(bipy)(CO)_3Cl$ - covered working electrode, a platinum counter electrode and an Ag/AgCl (3 M KCl) reference electrode. As electrolyte 0.05 M TRIS-buffer (pH 7.88, adjusted with 3 M HCl) was used. After saturating the system with N_2 or CO_2 respectively, cyclic voltammetry was measured between 0 and -1800 mV with a scan rate of 25 or 40 mV s^{-1}. For controlled potential electrolysis the potential was held for 3 h at -1600 mV. Product concentrations were determined with gas and ion chromatography.

As a proof of concept, same matrix was also used with a different electrode material - carbon felt. Electrode preparation as well as CV, electrolysis and product analytics were performed in the same way as for SiC substrates as described above.

3. Results and Discussion

3.1. Characterization of Wafers

3.1.1. Spectroscopic Characterization

Due to interband transitions, N-doped SiC samples of different polytype exhibit well-known colors: the 6H polytype appears green, while the 4H polytype is of greenish-yellow color (see Figure 1a).[46]

Intraband absorptions are due to free carriers. The measured UV-Vis - absorption spectra are shown in Figure 15.
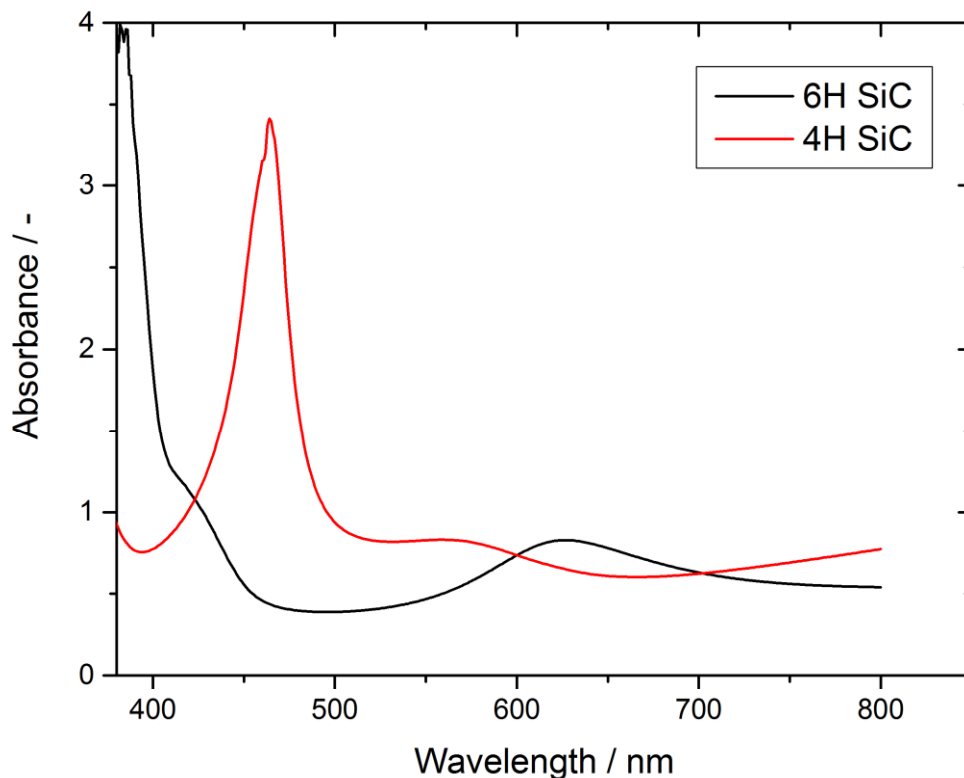
Figure 15: UV-Vis absorption of 4H- and 6H-SiC.

3.1.2. Electrical Characterization

A linear current-voltage relation could be proven by the ohmic check for both SiC polytypes as shown in Figure 16. Both linear fits show a correlation of 1.00. Therefore the contact formed by evaporating and annealing Ni on top is ohmic and can be used to address the electrodes for electrochemical applications.
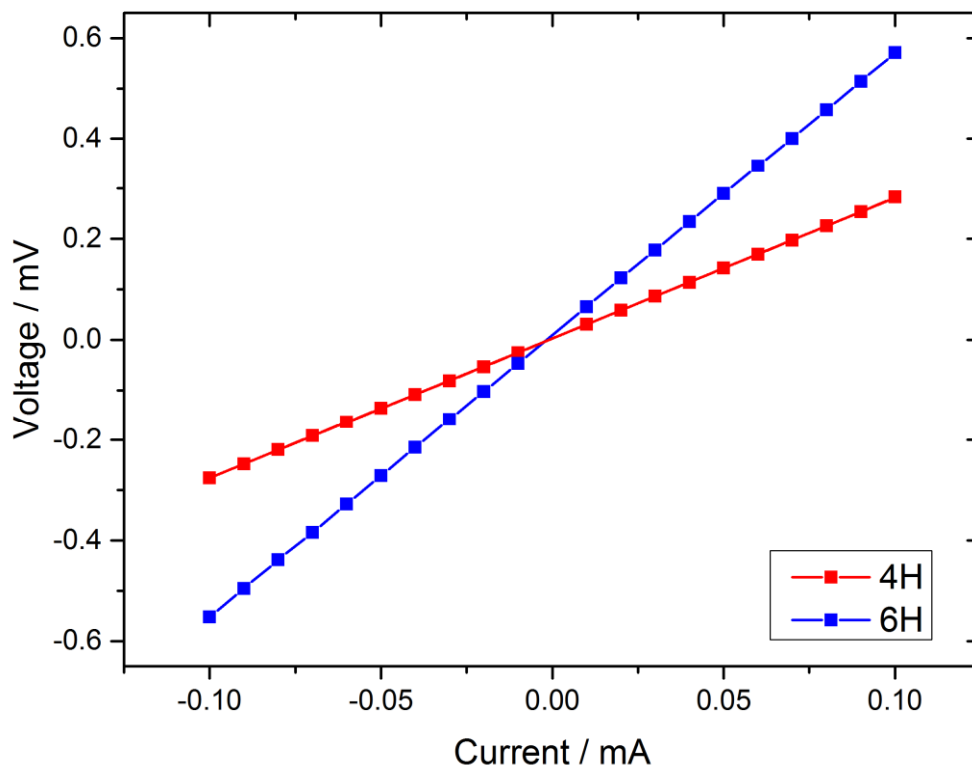
Figure 16: Current voltage relationship in 6H- and 4H-SiC.

By Hall measurement, doping concentrations of 7.08×10^{18} cm^{-3} for 4H-SiC and 1.74×10^{18} cm^{-3} for the 6H-SiC were determined. All other results are summarized in Table 7.

	4H-SiC	6H-SiC
carrier type	N	N
Hall mobility / cm^2 V^{-1} s^{-1}	5.76×10^1	8.04×10^1
Sheet carrier concentration / cm^{-2}	2.48×10^{17}	6.08×10^{16}
Hall coefficient / cm^{2}C^{-1}	8.82×10^{-1}	3.59×10^0
Resistivity / Ω cm^{-1}	1.53×10^{-2}	4.47×10^{-2}
sheet resistivity / Ω	4.37×10^{-1}	1.28×10^0
Hall voltage / V	1.60×10^{-6}	6.53×10^{-6}

Table 7: Results of the Hall measurement of 4H- and 6H-SiC.

3.1.3. Electrochemical Characterization

Both, the wafers and the porous SiC electrodes were characterized in aqueous electrolytes of different pH as well as acetonitrile. The supporting electrolytes were Na_2SO_4 or $TBAPF_6$ respectively. In Figure 17 cyclic voltammograms of 6H-SiC in N_2 atmosphere in the dark with different electrolytes are shown. The behavior is representative for wafer substrates of both polytypes. With decreasing pH, proton reduction is increasingly favored; therefore the reduction onset shifts to less negative values and the current increases. Current density in the measurement performed in organic, water-free electrolyte is very low, indicating stability of the electrode upon cathodic polarization, which has also been found by other groups.[47][35]
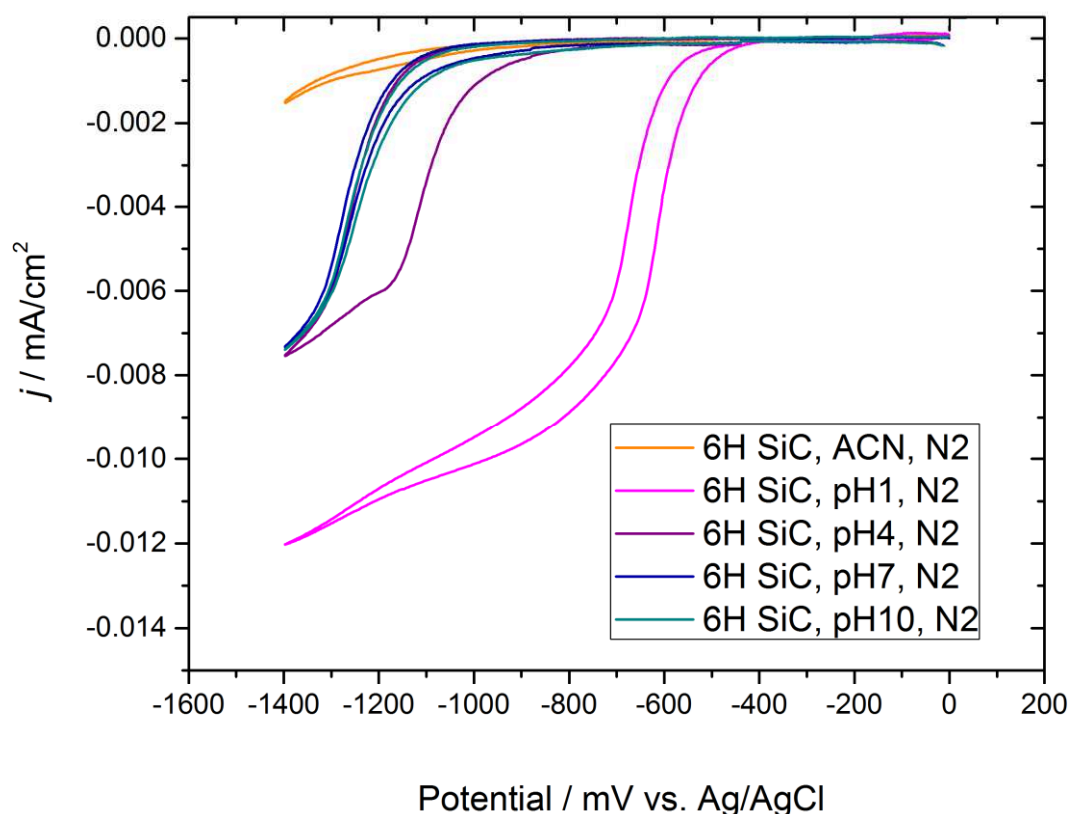
Figure 17: Cyclic voltammograms recorded with 6H-SiC as working electrode in various electrolytes saturated with N_2.

Same can be seen in a system, in which a porous SiC substrate is employed as the working electrode as shown in Figure 18. Lowering of pH increases the current and shifts the onset to less negative potentials. Due to the highly porous structure, capacitive current is dominating the measurements.
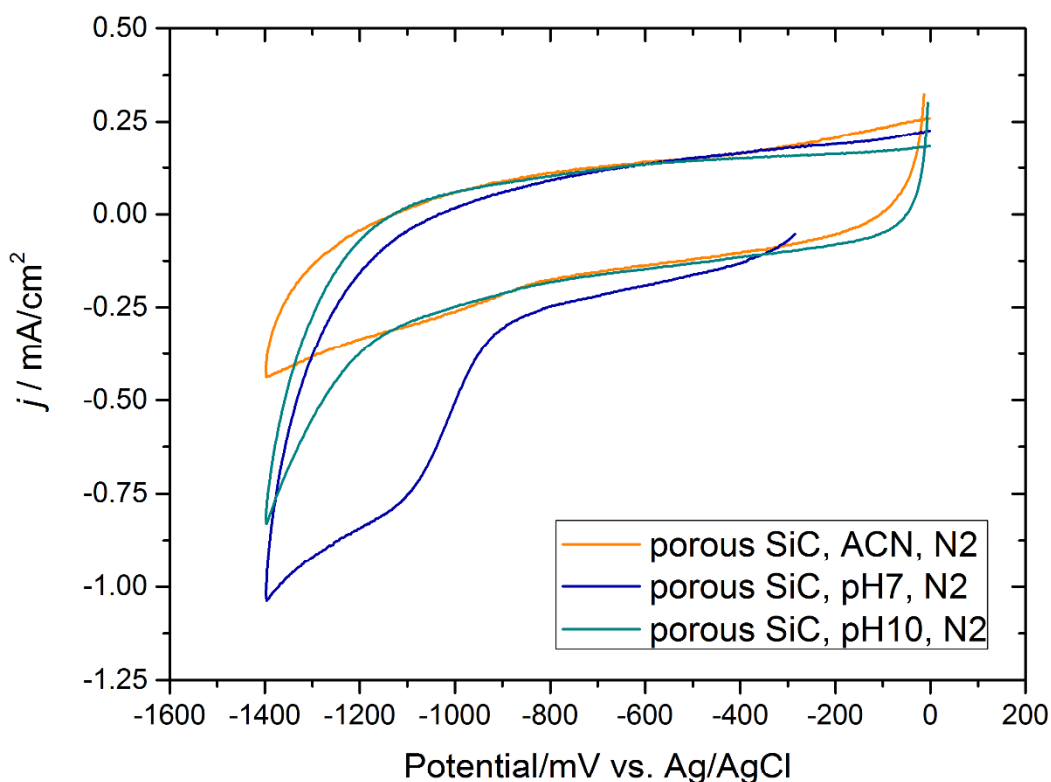
Figure 18: Cyclic voltammograms recorded with porous SiC as working electrode in various electrolytes saturated with N_2.

No light effect is apparent for the electrodes, neither for the porous nor for the wafer samples, neither in aqueous nor in organic solvents. Examples are shown in Figure 19 and Figure 20. This could be due to the fact that the samples are highly n-doped. For photoelectrochemical application as a cathode, a p-type material would be preferable[41][48], however this is not commercially available. Production of p-type material by the sol gel method is challenging and the products are not yet ready for application as an electrode.

Moreover, there is no noticeable catalytic activity towards CO_2 reduction. Cyclic voltammograms were recorded in all mentioned electrolytes in the N_2 saturated system as well as in the CO_2 saturated case. As can be seen in Figure 19, neither an increase in current nor an onset shift can be noticed in organic electrolyte indicating no catalytic activity. For the measurement in aqueous solvent (Figure 20), a slight onset shift can be detected, however analysis of the products of controlled potential electrolysis proved that this is only due to the pH-change to more acidic values upon CO_2 purging and therefore increased hydrogen evolution.
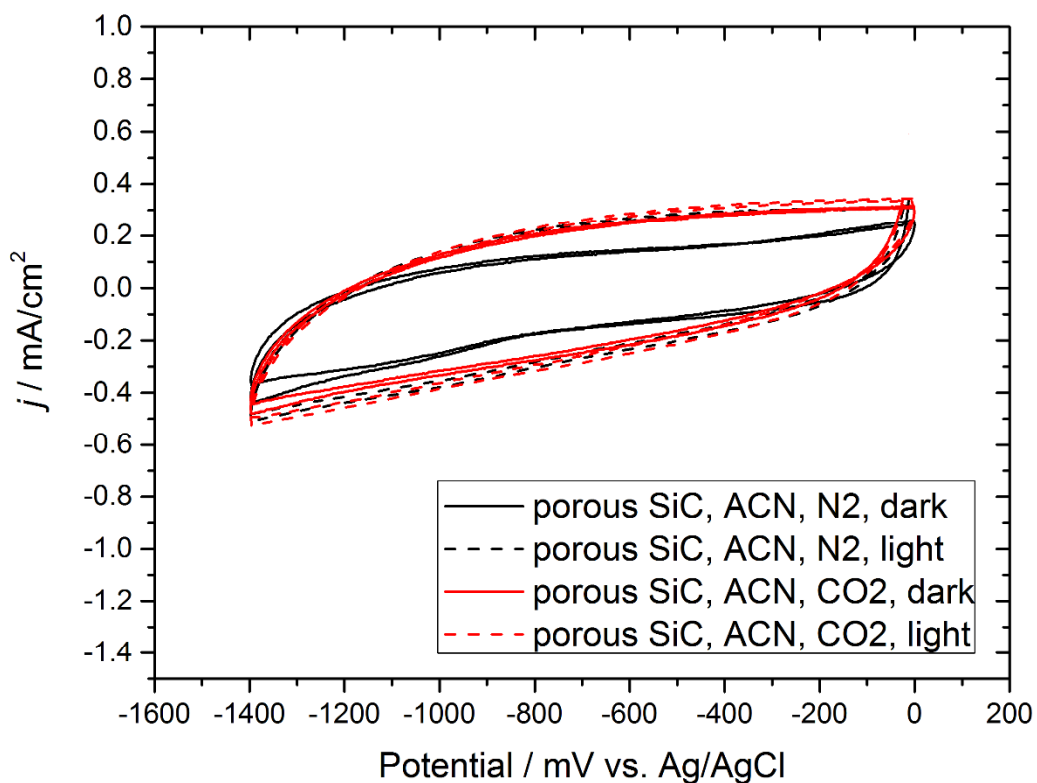
Figure 19: Cyclic voltammograms recorded with porous SiC as working electrode in acetonitrile with 0.1 M TBAPF$_6$ as supporting electrolyte saturated with N$_2$ or CO$_2$ respectively. CVs were recorded in the dark and upon illumination.
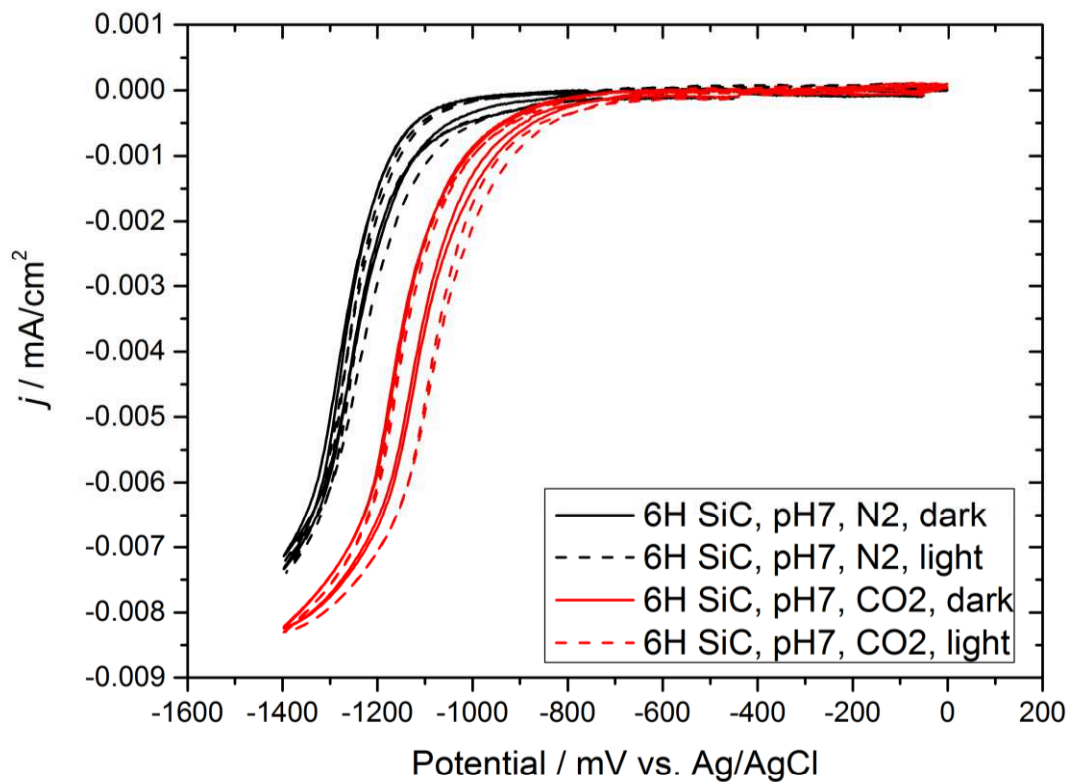
Figure 20: Cyclic voltammograms recorded with 6H-SiC as working electrode in 0.1 M Na$_2$SO$_4$ aqueous electrolyte saturated with N$_2$ or CO$_2$ respectively. CVs were recorded in the dark and upon illumination.

3.2. Homogeneous Enzyme Catalysis

To characterize a system in which formate dehydrogenase was employed as a homogeneous catalyst, cyclic voltammograms were recorded. Examples for an experiment with the wafer and the porous SiC electrodes are shown in Figure 21 and 22. Both feature neither an increase in cathodic current upon CO_2 saturation nor a distinct onset shift to less negative potentials. During controlled potential electrolysis an increase of formate over a period of 3 h could not be detected. Therefore catalytic activity of the enzyme seems to be negligible.
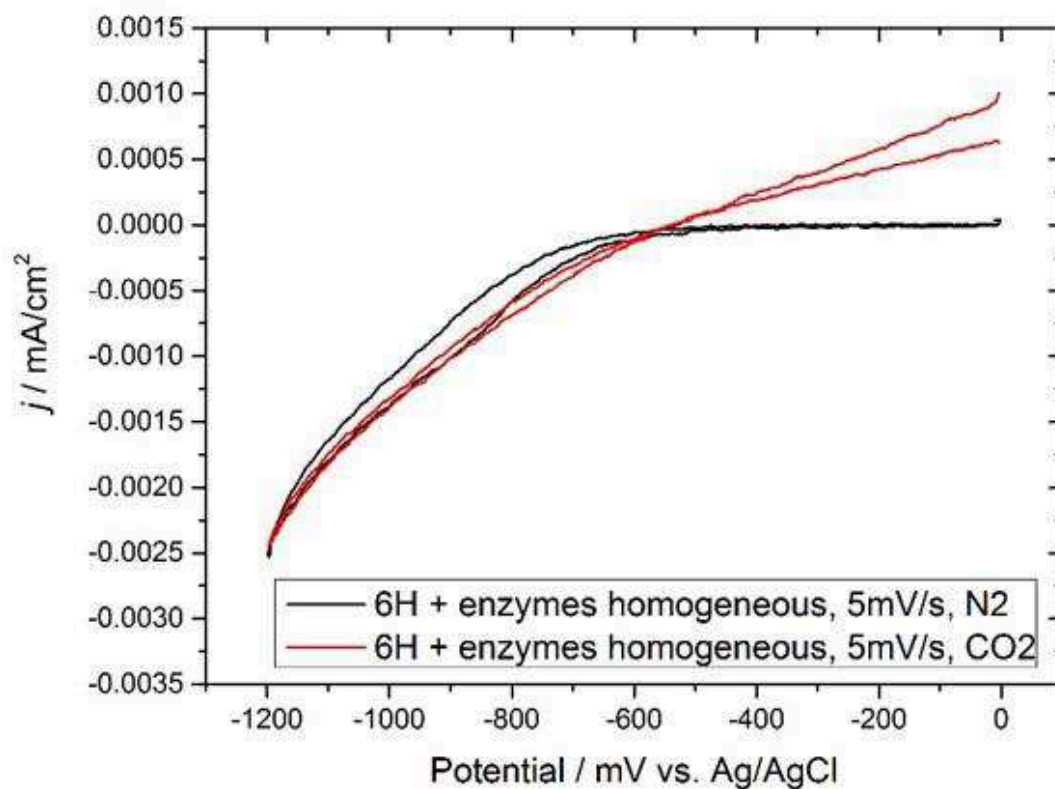
Figure 21: Cyclic voltammogram for a system, in which 6H-SiC represented the working electrode and formate dehydrogenase was used as a homogeneous catalyst.
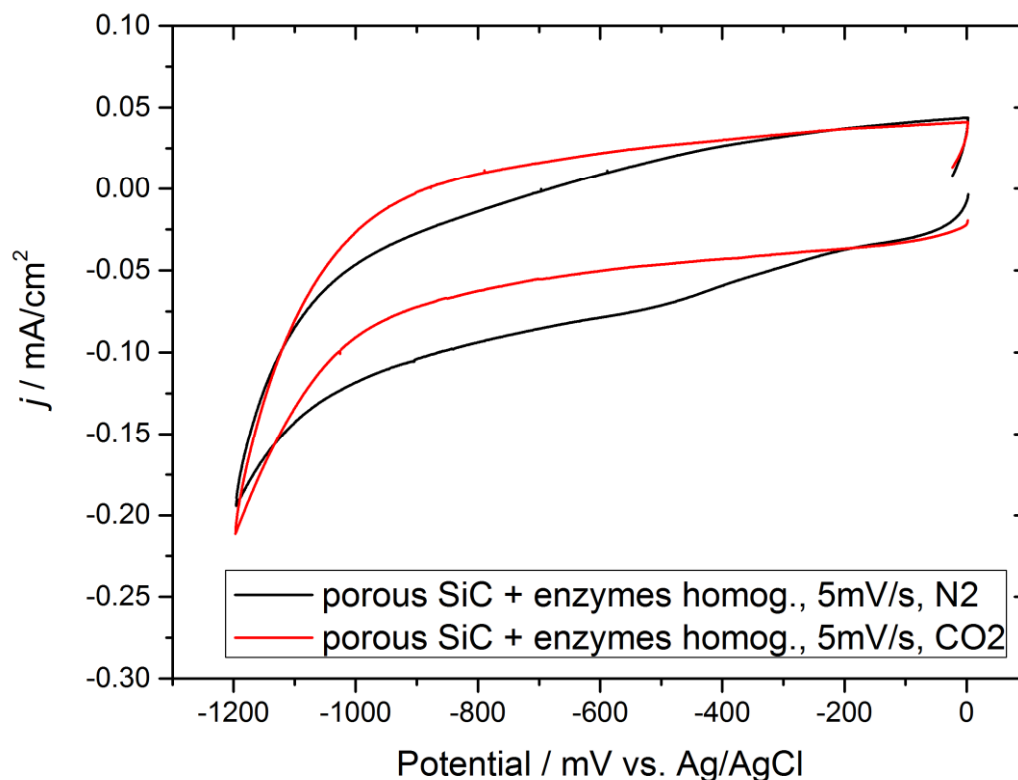
Figure 22: Cyclic voltammogram for a system, in which porous 3C-SiC represented the working electrode and formate dehydrogenase was used as a homogeneous catalyst.

In order to exclude the inactivity of the enzyme itself in the present environment as a possible problem, enzymatic activity testing in TRIS-buffer was performed. The reaction underlying the enzymatic activity test is depicted in Figure 23 whereas the results of the UV-Vis-adsorption measurement are shown in Figure 24. From the increase in the absorption at 340 nm corresponding to the NADH produced while the reaction proceeds, an enzymatic activity of ~0.19 U / mg could be calculated. Thus, the enzyme is active in TRIS-buffer.
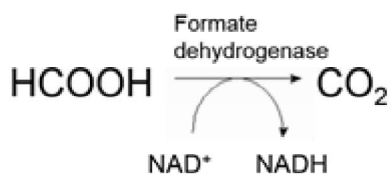
Figure 23: The reaction proceeding while the enzymatic activity test is performed.
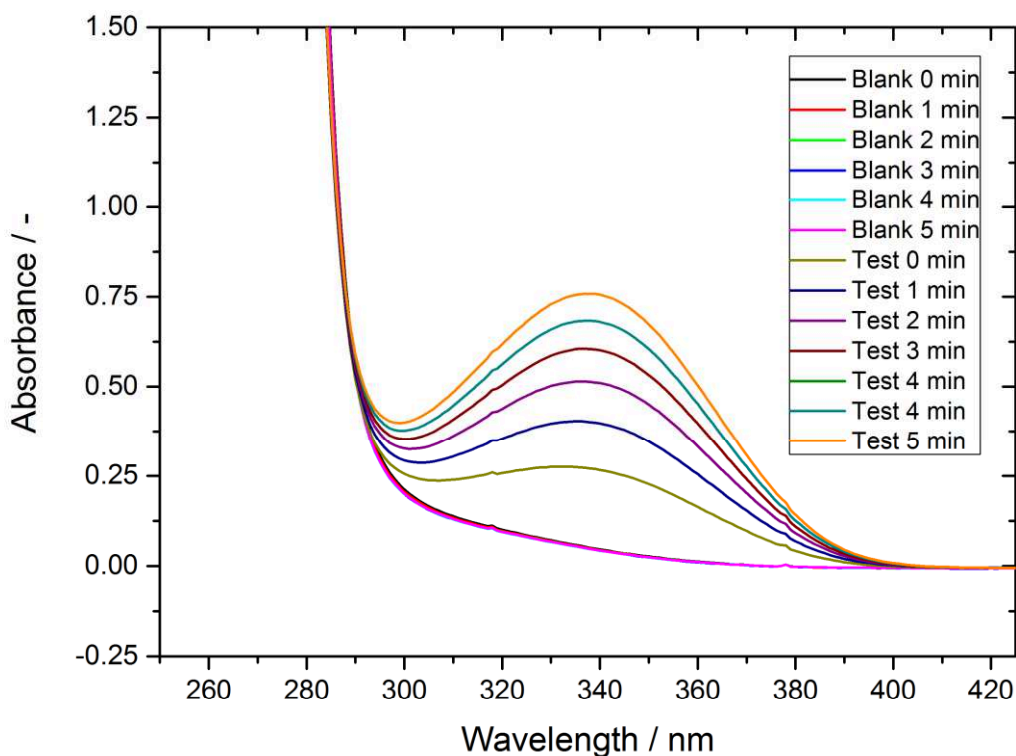
Figure 24: UV-Vis-spectra resulting from the enzymatic activity test with formate dehydrogenase in TRIS-buffer.

A possible explanation for the seemingly ineffective addressing of the enzyme by the SiC electrodes could be the missing metal center in commercially available formate dehydrogenase, typical for NAD-dependent enzymes.[49][21] The mechanism for electrochemical addressing of enzymes is still unclear but it is proposed that the electrons are first transferred to the metal active center.[21][6][25][26] The missing metal center in the enzymes used might complicate or hinder direct electron injection.

Another possible factor for the ineffectiveness of the homogenous system could be insufficient charge transport. Therefore, neutral red was employed as an electron shuttle in the system with a concentration of 10 mM, however there was still no detectable formate production achieved. As a next step heterogeneous catalysis by immobilization of the enzyme in an alginate silicate matrix was tested.

3.3. Heterogeneous Enzyme Catalysis

Heterogeneous enzyme catalysis was performed by immobilizing the enzyme in an alginate-silicate matrix on the electrode surface. As already mentioned above, experiments could only be carried out with porous 3C-SiC, since matrix delamination presented as inevitable problem with the wafers as substrates. The system was characterized by cyclic voltammetry as shown in Figure 28. In this case, the CO_2 saturated system exhibits lower currents than the system in nitrogen atmosphere. Therefore no catalytic activity is indicated even though charge transport and direct electron injection should be facilitated by the matrix. Considering that CV might not be the right technique for characterization of said system due to kinetic limitations of the slow conversion rate catalyst and low diffusion rate [24], controlled potential electrolysis was performed to verify the assumption of no catalytic activity. Consequently, even over a period of 3 h no reproducible, detectable amount of formate was formed.

As already discussed for the homogeneous case, a possible explanation could be the missing metal-center, which is believed to facilitate electron uptake from the electrode. [21][6][25][26].

Another potential reason could be that electron transfer from SiC to formate dehydrogenase might not be favorable, due to intrinsic properties of SiC. Especially taking into account that addressing same enzyme with a carbon felt electrode was achieved before, albeit with low efficiencies compared to other enzymes[24], one might consider SiC not being a well-suited substrate for electrochemically addressing formate dehydrogenase.
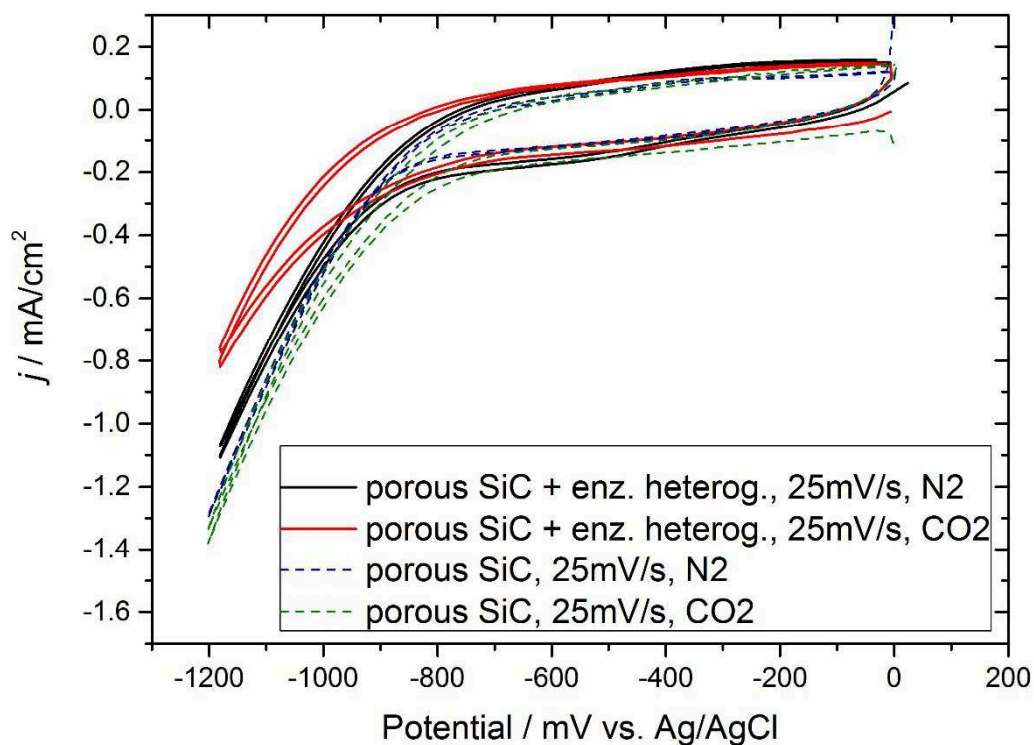
Figure 25: Cyclic voltammogram of porous 3C-SiC covered with immobilized enzyme.

3.4. Homogeneous Catalysis with Re(bipy)(CO)₃Cl

It is very well possible to address the benchmark catalyst Re(bipy)(CO)₃Cl with a SiC electrode as can be concluded from the characteristic shape of the cyclic voltammogram (see 1.4.) [10]. For comparison, the homogeneous catalysis system was characterized with each, SiC and Pt, as a
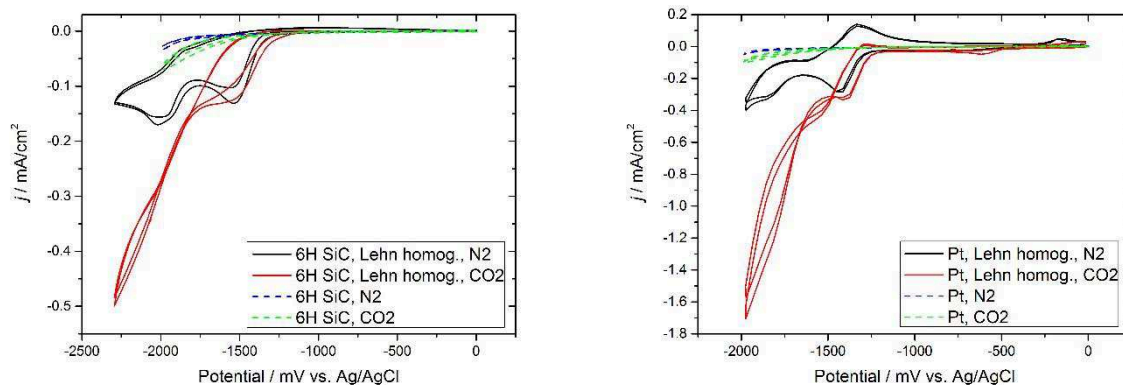
Figure 26: Cyclic voltammogram of a system, in which Re(bipy)(CO)₃Cl is employed as a homogenous catalyst and SiC (left) and platinum respectively (right) is used as the working electrode.

working electrode and in both, the N_2 saturated and the CO_2 saturated case. The results are depicted in Figure 29.

The required potential for reduction undergoes a negative shift of about 250 mV for the application with a SiC working electrode compared to the Pt case. Nevertheless, catalytic current is clearly indicated. Controlled potential electrolysis gives CO and formate as CO_2 reduction products as known from literature.[12][50][31]

It is also well known, that the addition of certain amounts of water increases the performance of the catalyst.[12] It could be shown that this trend is also true for the application of a SiC electrode. Therefore 0.5 - 5 % of 18.2 MΩ cm water were added to the electrolyte and cyclic voltammetry as well as controlled potential electrolysis was performed. CVs as well as faradaic efficiencies are shown in Figure 30 and Figure 31.
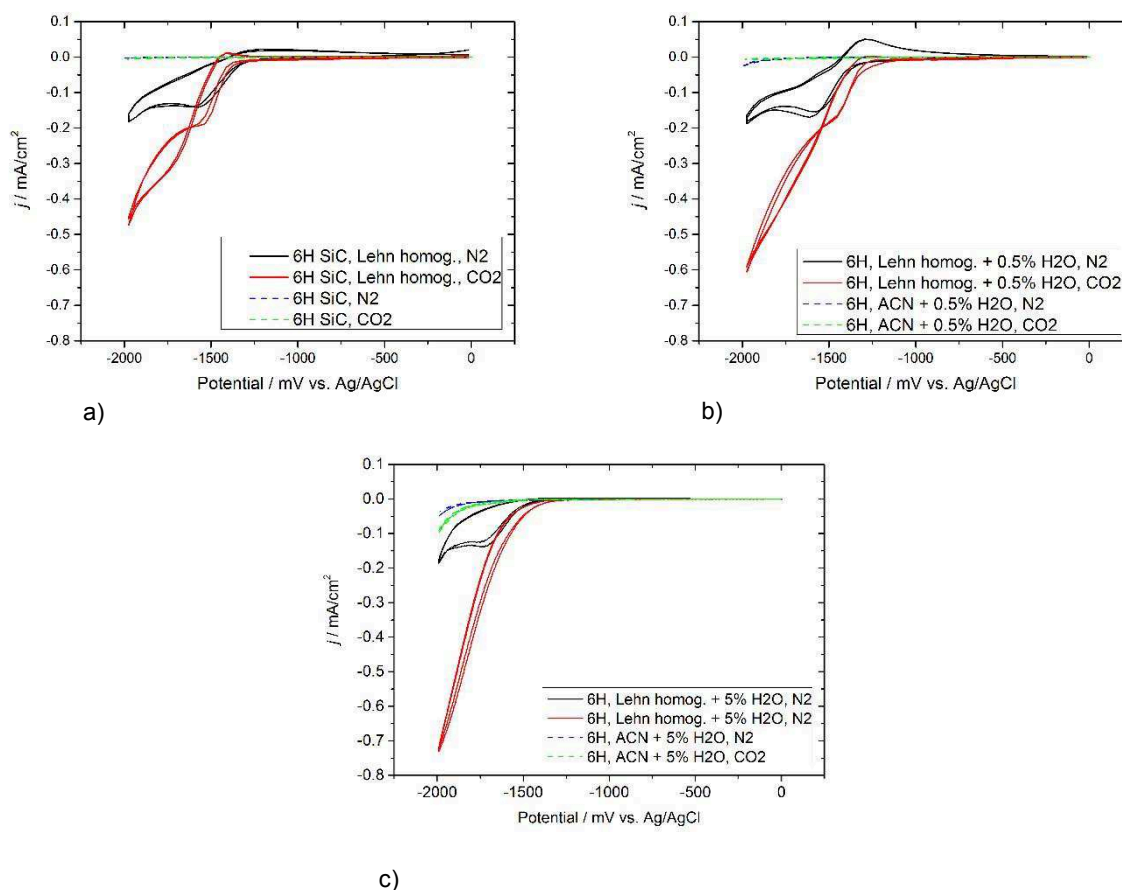
Figure 27: Cyclic voltammograms recorded with Re(bipy)(CO)₃Cl employed as a homogenous catalyst, 6H-SiC employed as the working electrode and a) 0 %, b) 0.5% or c) 5 % water addition to the organic electrolyte.
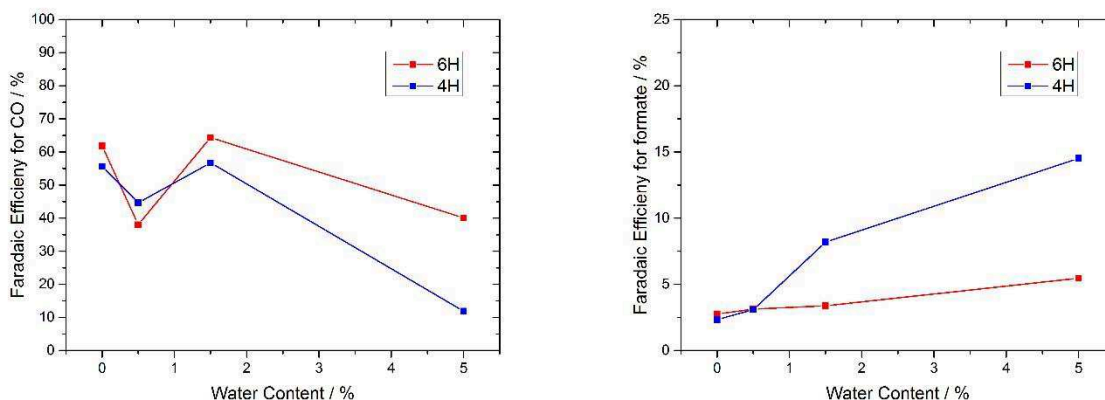
Figure 28: Faradaic efficiencies for CO (left) and formate (right) determined according to product amounts after 3 h electrolysis.

Not only can one notice an increase of the current with increasing water amount but also distinct trends for faradaic efficiency. While the CO production decreases after reaching a maximum at 1.5 %, the formate production continuously increases. This arouses interest for using the catalyst in aqueous environment, since formate as a valuable chemical (see 1.1.1.) is definitely a targeted product for CO_2 reduction.

3.5. Heterogeneous Catalysis with Re(bipy)(CO)$_3$Cl

To overcome solubility issues[32] (see Figure 32) and use Re(bipy)(CO)$_3$Cl in aqueous environment, in a novel approach the catalyst was immobilized in the alginate-silicate matrix.

Figure 29: The hydrophobic catalyst Re(bipy)(CO)$_3$Cl is not soluble in water, therefore homogenous approaches are only possible in organic electrolytes.

The system was then characterized with cyclic voltammetry as can be seen in Figure 33. A clear onset shift of 170 mV to less negative potentials in the CO_2 saturated system, as well as increased current indicate catalytic activity. Due to diffusion limitations, some capacitive current was observed as well.
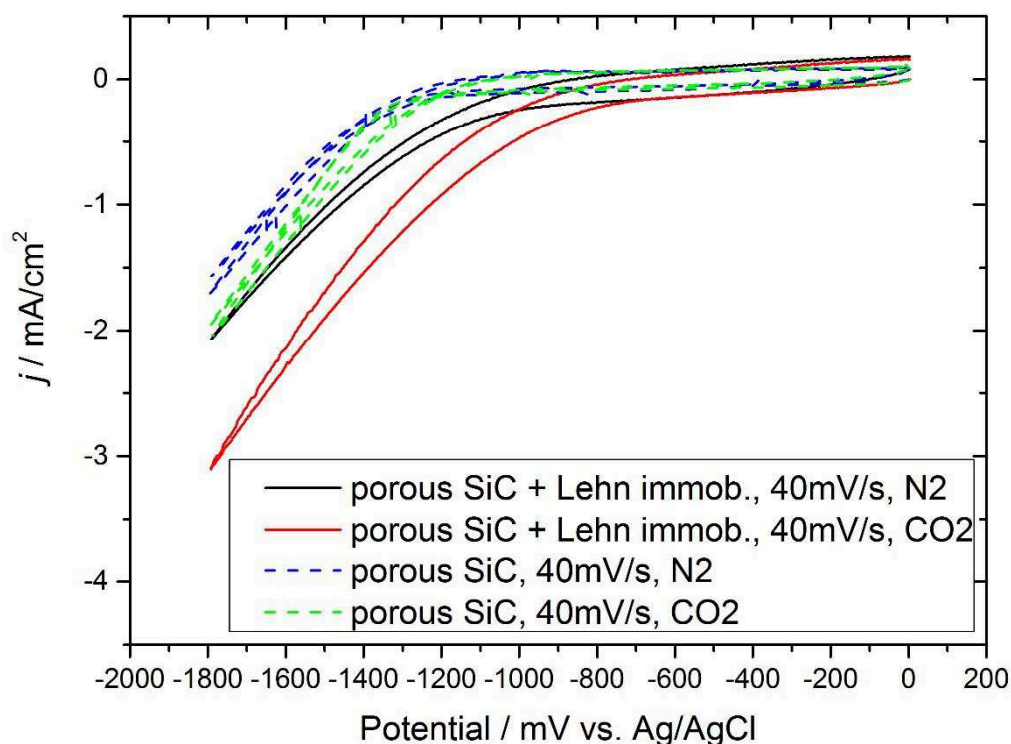
Figure 30: Cyclic voltammogram of a system, in which SiC covered with Re(bipy)(CO)₃Cl immobilized in alginate-silicate matrix was employed as a working electrode in aqueous environment.

To further prove the catalyst being active in this matrix, controlled potential electrolysis was run at -1600mV for the N_2 saturated system and for the CO_2 saturated system respectively. For first electrolysis experiments, a rather high overpotential to the thermodynamic formal potential of $E^{0'} = -0.61$ V was applied, since formate is known to often require high overpotentials.[1] The current density over time for a 3 h period is depicted in Figure 34. The current observed in the case of the N_2 saturated system originates from hydrogen evolution, since proton reduction is inevitable if a potential of -1600 mV is applied in aqueous solvent. In the case of CO_2 saturation, cathodic current increased by a factor of ~2.5. Stable current flow lead to the conclusion of high catalyst stability even with applied potential. A reproducible faradaic efficiency of ~23 % for formate could be achieved with formate being the only CO_2-reduction product that could be detected. The only known side product is H_2. Therefore not only the utilization of the catalyst in

aqueous environment could be enabled, but moreover high selectivity for one specific product could be achieved. Due to the heterogeneous approach catalyst reusability and separation from the product is facilitated. In comparison to previous studies making use of catalyst immobilization in Nafion membrane [32][31], high current densities could be achieved.
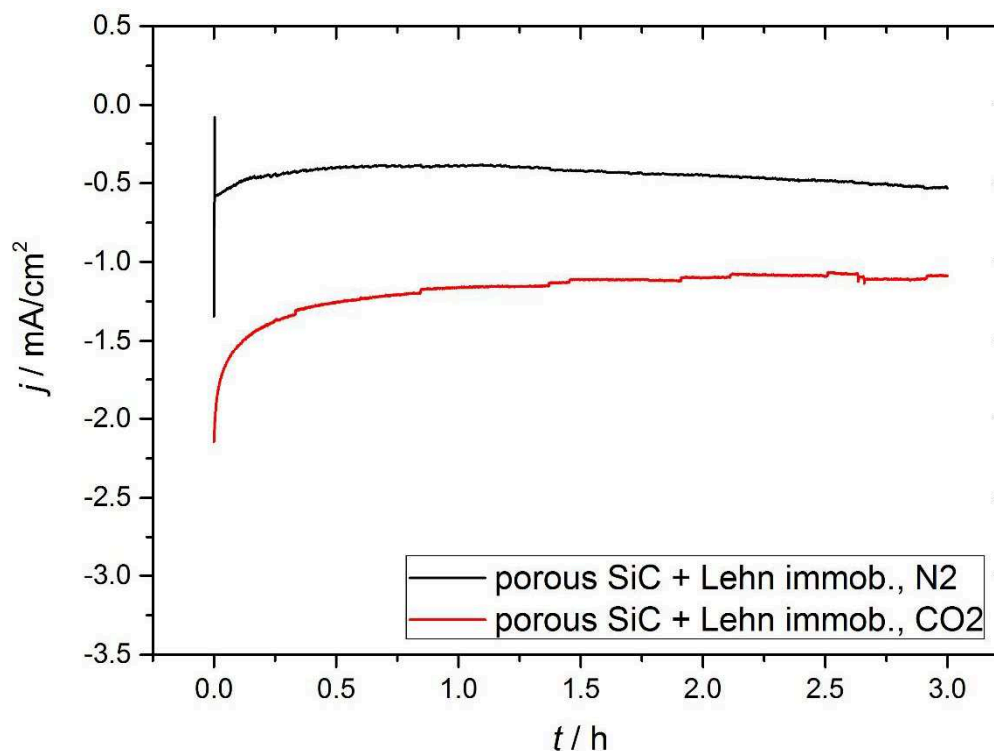
Figure 31: Current density over time for a 3 h electrolysis period of a system, in which SiC covered with Re(bipy)(CO)$_3$Cl immobilized in alginate-silicate matrix was employed as a working electrode in aqueous environment.

As a proof of concept, same matrix was also tested with another electrode material - carbon felt. Characterization was again achieved by cyclic voltammetry experiments as well as by controlled potential electrolysis. The results are shown in Figure 35 and Figure 36. Again an onset shift of ~170mV to less negative values, as well as an increase of current could be observed. Therefore at least a part of the immobilized catalyst amount is still active towards CO_2 reduction. Consequently immobilization of the catalyst in the alginate-silicate matrix could be proven to be effective. Nevertheless, porous SiC seems to be the favorable choice as a substrate since hydrogen evolution is the dominating reaction at a carbon felt substrate leading to a low faradaic efficiency of 2.1 % towards formate.
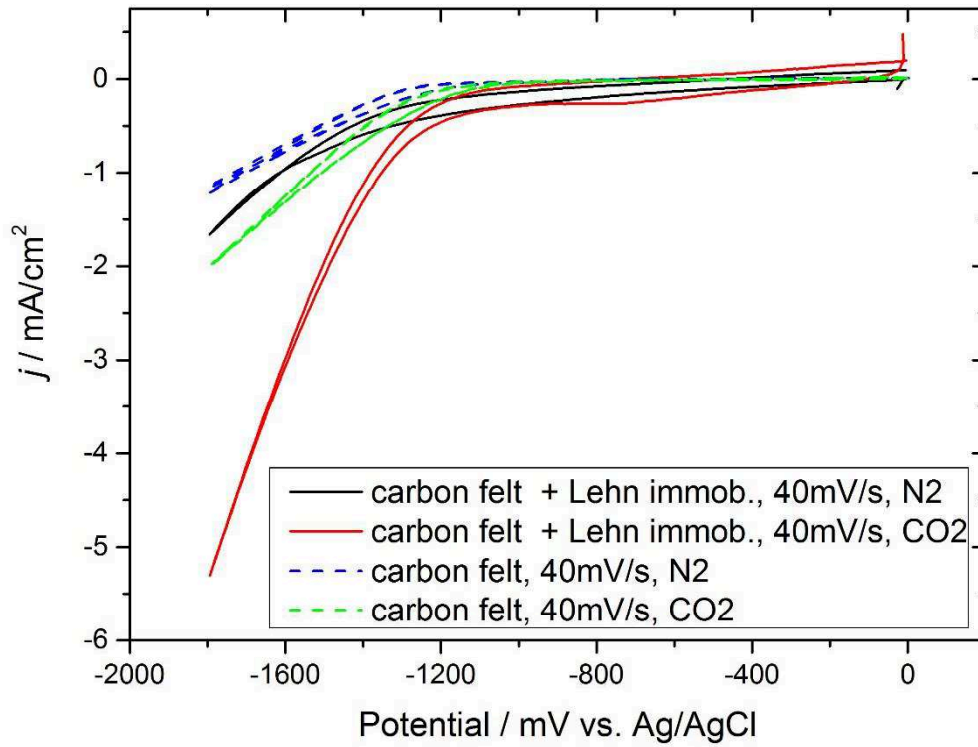
Figure 32: Cyclic voltammogram of a system, in which carbon felt covered with Re(bipy)(CO)$_3$Cl immobilized in alginate-silicate matrix was employed as a working electrode in aqueous environment.
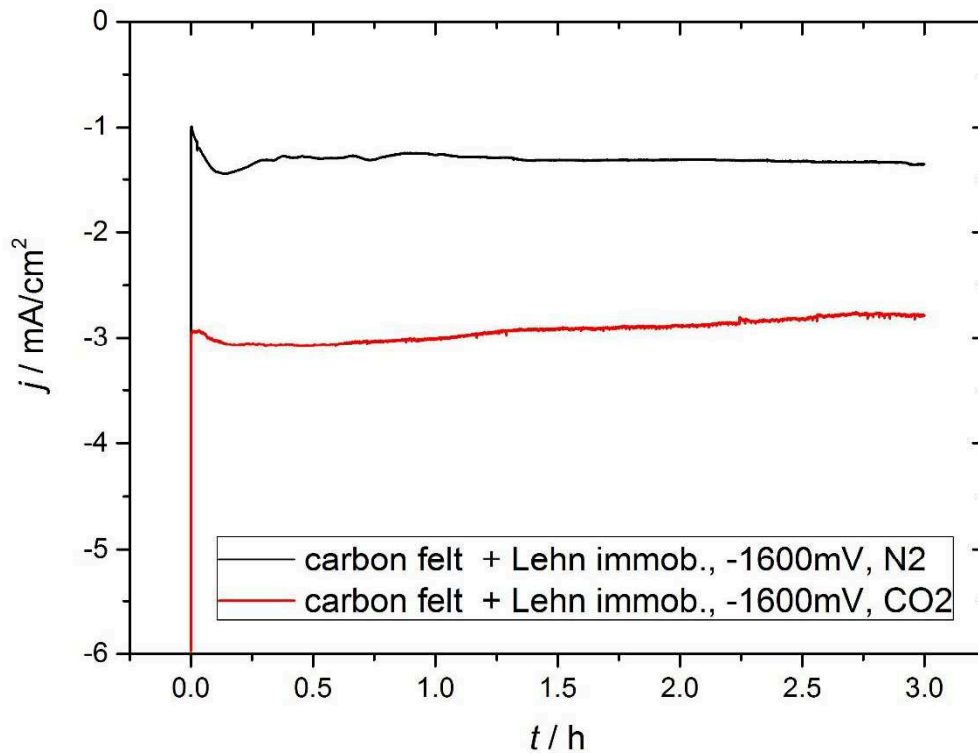
Figure 33: Current density over time for a 3 h electrolysis period of a system, in which carbon felt covered with Re(bipy)(CO)$_3$Cl immobilized in alginate-silicate matrix was employed as a working electrode in an aqueous environment.

4. Conclusion and Outlook

In this thesis it could be shown that silicon carbide of different polytypes, monocrystalline or polycrystalline and porous or non-porous can be employed as an electrode for electrocatalytic CO_2 reduction in aqueous as well as organic electrolytes.

The compatibility with the biocatalyst formate dehydrogenase seemed limited, which could be a result of hindered direct electron injection due to the missing metal center of the enzyme. Neither for the homogenous nor for the heterogeneous approach a reproducible and detectible amount of CO_2 reduction products could be achieved. For heterogeneous catalysis with immobilization of the enzyme in an alginate-silicate matrix, the wafers did not present the ideal substrate due to surface delamination. However inexpensive porous silicon carbide electrodes fabricated by a sol-gel process display well-suited surface properties for modification with the alginate-silicate hybrid gel.

In contrary to the enzyme the organometallic benchmark compound Re(bipy)(CO)$_3$Cl could be properly addressed in electrochemical experiments. Homogeneous catalysis in organic electrolytes with or without the addition of a protic solvent was proven to be effective towards CO_2 reduction. Due to the observed trend of rising faradaic efficiencies for the valuable product formate upon increasing content of a protic solvent, using the catalyst in pure aqueous electrolyte was of interest. Due to solubility issues, a heterogeneous approach was necessary. Therefore the catalyst was immobilized on the electrode with alginate-silicate hybrid gel. While said matrix is well known for the immobilization of enzymes, it was shown that the application of such for the organometallic benchmark catalyst Re(bipy)(CO)$_3$Cl can be realized in aqueous solution. With this new way of utilization electrocatalytic CO_2 reduction to formate with high product selectivity could be achieved. Future experiments should focus on optimizing the potential and other electrolysis conditions to further improve the efficiency for this system.

In this thesis only n-type SiC was investigated, due to availability issues of p-type material. Therefore no light effect in the reductive range could be detected. Nevertheless all systems investigated offer the prospective for photoelectrochemical application as soon as p-type material can be efficiently synthesized by the sol gel method or provided by other manufacturers.

Acknowledgements

First of all, I would like to express my gratitude to Professor Sariciftci for giving me the chance and honor to work in the inspiring and motivating environment, which he created at LIOS. Being surrounded by so many great researchers provides constant encouragement for giving one's best for science every day.

A very special thank you goes to Dogukan Hazar Apaydin for being a patient teacher and supervisor, for introducing me to the field of CO_2-reduction and many techniques related to said topic, for his guidance through the whole process of preparing this thesis and last but not least for his support with new ideas always encouraging creativity and innovation.

Next, I owe gratitude to Bettina Friedel and Olivia Kettner for providing 3C-SiC samples and Herwig Heilbrunner for Hall measurement.

Finally, I would like to thank my colleagues Gabriele Hinterberger, Stefanie Schlager, Liviu Dumitru, Patrick Whang and Christoph Ulbricht, just to mention some, for valuable advice and inspiring discussions.

List of Figures

List of Tables

References

[1]   M. Aresta, *Carbon Dioxide as Chemical Feedstock*, Wiley-VCH, Weinheim, **2010**.

[2]   M. Aresta, *Coordination Chemistry Reviews* **2016**, *in press*.

[3]   S. Rackley, *Carbon capture and storage*, Academic, Oxford, **2009**.

[4]   Wilson G., Armstrong K., Saussez G., Travaly Y., Bolscher H., Knippels H., Brun T., Krämer D., Rothengatter N., Styring P., Veenstra E., Buck L., Mooney J., *A strategic European resarch and innovation agenda for smart CO2 transformation in Europe*, **2016**.

[5]   J. L. White, M. F. Baruch, J. E. Pander Iii, Y. Hu, I. C. Fortmeyer, J. E. Park, T. Zhang, K. Liao, J. Gu, Y. Yan et al., *Chemical reviews* **2015**, *115*, 12888–12935.

[6]   A. M. Appel, J. E. Bercaw, A. B. Bocarsly, H. Dobbek, D. L. DuBois, M. Dupuis, J. G. Ferry, E. Fujita, R. Hille, P. J. A. Kenis et al., *Chemical reviews* **2013**, *113*, 6621–6658.

[7]   B. Kumar, M. Llorente, J. Froehlich, T. Dang, A. Sathrum, C. P. Kubiak, *Annual review of physical chemistry* **2012**, *63*, 541–569.

[8]   E. E. Benson, C. P. Kubiak, A. J. Sathrum, J. M. Smieja, *Chemical Society reviews* **2009**, *38*, 89–99.

[9]   M. Aresta, A. Dibenedetto, E. Quaranta, *Journal of Catalysis* **2016**.

[10]   E. Portenkirchner, K. Oppelt, C. Ulbricht, D. A. Egbe, H. Neugebauer, G. Knör, N. S. Sariciftci, *Journal of Organometallic Chemistry* **2012**, *716*, 19–25.

[11]   S. Schlager, H. Neugebauer, M. Haberbauer, G. Hinterberger, N. S. Sariciftci, *ChemCatChem* **2015**, *7*, 967–971.

[12]   Hawecker, Lehn, Ziessel, *Helvetica Chimica Acta* **1986**, 1990–2012.

[13]   A. S. Agarwal, Y. Zhai, D. Hill, N. Sridhar, *ChemSusChem* **2011**, *4*, 1301–1310.

[14]   F. Joo, *ChemSusChem* **2008**, *1*, 805–808.

[15]   C. Fellay, P. J. Dyson, G. Laurenczy, *Angewandte Chemie (International ed. in English)* **2008**, *47*, 3966–3968.

[16]   C. Fellay, N. Yan, P. J. Dyson, G. Laurenczy, *Chemistry (Weinheim an der Bergstrasse, Germany)* **2009**, *15*, 3752–3760.

[17]   X. Yu, P. G. Pickup, *Journal of Power Sources* **2008**, *182*, 124–132.

[18]   C. Rice, S. Ha, R. I. Masel, P. Waszczuk, A. Wieckowski, T. Barnard, *Journal of Power Sources* **2002**, *111*, 83–89.

[19]   R. A. Sheldon, *Adv. Synth. Catal.* **2007**, *349*, 1289–1307.

[20]   C. Mateo, J. M. Palomo, G. Fernandez-Lorente, J. M. Guisan, R. Fernandez-Lafuente, *Enzyme and Microbial Technology* **2007**, *40*, 1451–1463.

[21]   J. Shi, Y. Jiang, Z. Jiang, X. Wang, X. Wang, S. Zhang, P. Han, C. Yang, *Chemical Society reviews* **2015**, *44*, 5981–6000.

[22] S.-w. Xu, Y. Lu, J. Li, Z.-y. Jiang, H. Wu, *Ind. Eng. Chem. Res.* **2006**, *45*, 4567–4573.

[23] R. Obert, B. C. Dave, *J. Am. Chem. Soc.* **1999**, *121*, 12192–12193.

[24] S. Schlager, *Biocatalytic and Bio-electrocatalytic Reduction of CO2 using Enzymes and Microogranisms*, **2015**.

[25] T. Reda, C. M. Plugge, N. J. Abram, J. Hirst, *Proceedings of the National Academy of Sciences of the United States of America* **2008**, *105*, 10654–10658.

[26] A. Bassegoda, C. Madden, D. W. Wakerley, E. Reisner, J. Hirst, *Journal of the American Chemical Society* **2014**, *136*, 15473–15476.

[27] Schlager S., Dumitru L., Haberbauer M., Fuchsbauer A., Neugebauer H., Hiemetsberger D., Wagner A., Portenkirchmer E., Sariciftci N.S., *ChemSusChem* **9**, *2016*, 631–635.

[28] Y. Lu, Z.-y. Jiang, S.-w. Xu, H. Wu, *Catalysis Today* **2006**, *115*, 263–268.

[29] Hawecker J., Lehn J.M., Ziessel R., *J. Chem. Soc., Chem. Commun.* **1984**, 328–330.

[30] B. P. Sullivan, C. M. Bolinger, D. Conrad, W. J. Vining, T. J. Meyer, *J. Chem. Soc., Chem. Commun.* **1985**, 1414–1416.

[31] T. Yoshida, K. Tsutsumida, S. Teratani, K. Yasufuku, M. Kaneko, *J. Chem. Soc., Chem. Commun.* **1993**, 631–633.

[32] J. J. Walsh, G. Neri, C. L. Smith, A. J. Cowan, *Chemical communications (Cambridge, England)* **2014**, *50*, 12698–12701.

[33] T. Kimoto, *Fundamentals of Silicon Carbide Technology*, Wiley, Singapore, **2014**.

[34] Bettina Friedel, *3C-SiC auf Sol-Gel-Basis. Entwicklung, Wachstumsechanismen und Charakter anwendungsorientierter Morphologien des Wide-Bandgap-Halbleiters*. Dissertation, Paderborn, **2007**.

[35] N. Yang, H. Zhuang, R. Hoffmann, W. Smirnov, J. Hees, X. Jiang, C. E. Nebel, *Analytical chemistry* **2011**, *83*, 5827–5830.

[36] B. Friedel, S. Greulich-Weber, *MRS Proc.* **2008**, *1069*.

[37] S. Greulich-Weber, B. Friedel, *MSF* **2009**, *615-617*, 637–640.

[38] B. Friedel, S. Greulich-Weber, *MSF* **2006**, *527-529*, 759–762.

[39] A. J. Bard, L. R. Faulkner, *Electrochemical methods. Fundamentals and applications,* 2. Aufl., Wiley, New York, **2001**.

[40] P. T. Kissinger (Hrsg.) *Laboratory techniques in electroanalytical chemistry. Chapter 28*, Dekker, New York, NY, **1996**.

[41] L. M. Peter in *RSC Energy and Environment Series* (Hrsg.: J. Schneider, D. Bahnemann, J. Ye, G. Li Puma, D. D. Dionysiou), Royal Society of Chemistry, Cambridge, **2016**.

[42] L. M. Porter, R. F. Davis, *Materials Science and Engineering: B* **1995**, *34*, 83–105.

[43] R. Cheung (Hrsg.) *Silicon Carbide Microelectromechanical Systems for Harsh Environments*, Imperial College Press, **2006**.

[44] E. Portenkirchner, *Photoinduced Electron Transfer from Organic Semiconductors onto Redox Mediators for CO$_2$ Reduction*, Dissertation, Linz, **2014**.

[45] Sigma Aldrich, *Enzymatic Assay of Formate Dehydrogenase (EC 1.2.1.2.)*, **1996**.

[46] a) Y. Zhang, T. Xia, P. Wallenmeyer, C. X. Harris, A. A. Peterson, G. A. Corsiglia, J. Murowchick, X. Chen, *Energy Technology* **2014**, *2*, 183–187; b) Gary Haris, *Properties Of Silicon Carbide*, inspec, London, **1995**.

[47] Lauermann, Iver, Meissner, *J. Electrochem. Soc.* **1997**, *144*, 73.

[48] C. D. Windle, E. Pastor, A. Reynal, A. C. Whitwood, Y. Vaynzof, J. R. Durrant, R. N. Perutz, E. Reisner, *Chemistry (Weinheim an der Bergstrasse, Germany)* **2015**, *21*, 3746–3754.

[49] K. Schirwitz, A. Schmidt, V. S. Lamzin, *Protein science : a publication of the Protein Society* **2007**, *16*, 1146–1156.

[50] J.-M. Saveant, *Chemical reviews* **2008**, *108*, 2348–2378.

Curriculum Vitae

Contact details

- Kathrin Ebner
  Figulystraße 12
  4020 Linz
  Austria
- +43 (0) 677 61794774
- kathi.ebner@gmx.net

Personal Information

- born: 1.12.1992
- Citizenship: Austria

Education

- **Matura**
  Bundesgymnasium Enns.
  Graduated June 2011 with distinction.

- **Bachelor Studies in Technical Chemistry**
  Johannes Kepler University Linz, Thesis at the Institute of Analytical Chemistry
  (Head: o.Univ.Prof.DI Dr. Wolfgang Buchberger).
  Graduated July 2014 with distinction.

- **Master Studies in Technical Chemistry**
  Johannes Kepler University Linz, Thesis at the Institute of Physical Chemistry
  (Head: *o*.Univ. Prof. Mag. Dr. DDr. h.c. Niyazi Serdar Sariciftci).
  Expected to be graduating in November 2016.

Academic and Professional Positions

- 2012 - 2016: **Project "Frauen in die Technik"**
  Johannes Kepler University Linz.

- 2015: **Tutor**
  Johannes Kepler University Linz, Institute of Analytical Chemistry
  (Head: o.Univ.Prof.DI Dr. Wolfgang Buchberger).

- 2015: **Student Research Assistant**
  University of Montana, Department of Chemistry and Biochemistry
  (Head: Dr. Christopher Palmer).
  in the course of a semester studying abroad.

Conferences

- International Conference on Carbon Dioxide Utilization, September 2016:
  Poster Presentation and Flash Presentation: "Porous Silicon Carbide electrodes for catalytic reduction of carbon dioxide"

Awards

- Academic year 2013/2014: **Merit Scholarship - Faculty of Engineering and Natural Sciences**

- Academic year 2014/2015: **Merit Scholarship - Faculty of Engineering and Natural Sciences**

References

- **o.Univ. Prof. Mag. Dr. DDr. h.c. Niyazi Serdar Sariciftci**
  Head of the Linz Institute for Organic Solar Cells/ Institute of Physical Chemistry,
  Johannes Kepler University Linz.
  serdar.sariciftci@jku.at

- **Dr. Chris Palmer**
  Head of the Department of Chemistry and Biochemistry,
  University of Montana.
  christopher.palmer@umontana.edu